Russian Chemical Reviews **64**(7) 599–625 (1995)
©1995 Russian Academy of Sciences and Turpion Ltd

UDC 541.183+538.971

Molecular modelling of the chemical interaction of atoms and molecules with a surface

A A Valuev, A S Kaklyugin, G E Norman

Contents

I.	Introduction	599
II.	Classical molecular dynamics	600
III.	The regions of applicability of the adiabatic approximation	602
IV.	Adiabatic quantum molecular dynamics	604
V.	Reconstruction, adsorption, surface diffusion, clusters	605
VI.	Chemical reactions in terms of the adiabatic approximation	609
VII.	Nonadiabatic quantum molecular modelling	612
VIII.	Transition from dynamic to probability modelling	613
IX.	The simplest probability models. Cellular automata	614
X.	Quantum description of the chemical bond on the surface	615
XI.	The method based on the generalised periodic system of the elements	616
XII.	Results of the modelling of the modification of the surface	620

Abstract. **The modelling of a surface as an assembly of moving atoms interacting with one another and with an incident particle is examined. Both dynamic methods for the modelling of a surface (for short times) and probability methods (for long times) are analysed. The Massey adiabaticity criterion has been used to determine the regions of applicability of the methods of molecular dynamics. Within the framework of probability methods, the chemical bond is described with the aid of Harrison's generalised periodic system of the elements. Together with the general modelling problems, the reconstruction of the surface, physical and chemical sorption, as well as the modification of the surface and of its morphology as a result of the multiple repetition of elementary processes (precipitation, etching, corrosion) are discussed. The bibliography includes 169 references.**

I. Introduction

The molecular modelling of the chemical interaction of atoms and molecules with a surface is based on the concept of the surface as an assembly of moving individual atoms or molecules interacting with one another and with the incident particle.[1–6] The central problem is that of the description of the chemical bonds, including the situation where the incident particle interacts with the surface, at a level ensuring the reconstruction of the surface, the generation of electronic surface states, etc. Problems involving the selection of the laws of motion arise: the Newton and Schrödinger equations, the stochastic approximations of the type of Langevin equations, and the specification of the interactions between the particles. The next problem is that of the selection of the number of atoms, the geometry of their arrangement in the cell, and the boundary conditions representing the interaction of these atoms with the surrounding medium.

In the classical method of molecular dynamics (MMD), Newton's equations are solved numerically. The principal problem is that of selecting the interaction potential. In the quantum MMD, the interaction energy for each configuration of the heavy particles is found in the course of the calculation by solution of the Schrödinger equation. The observed forces acting on the ions are used to determine the classical trajectories of the latter.

Both the classical and the quantum MMD are valid only for a particular electronic state (the adiabatic approximation). Such approaches are suitable for the determination of equilibrium characteristics of different states and for modelling the dynamics within the framework of only one electronic state.

The adiabatic approximation is inapplicable in the region of the intersection of the potential surfaces of different electronic states. In these regions, the motion of the heavy particles may induce electronic transitions and their trajectories permit branching. The main problem involves the search for an effective solution of the nonstationary Schrödinger equation.[5] Modern computers permit calculations for times many orders of magnitude shorter than those required for the description of the dynamics of the modification of the surface in terms of real length and time scales. However, such problems generally require the consideration of nonadiabatic chemical reactions. This inevitably introduces a probability element into the dynamics. Furthermore, the dynamic memory of the initial conditions is retained only over periods of the order of magnitude of several relaxation times, after which the trajectories become stochastic, as happens in nature.[7–11]

For this reason, it is necessary to resort to probability modelling methods as well as dynamic methods, particularly since in many cases the result of a specific dynamic process and not the process itself is important. Discrete probability

A A Valuev, A S Kaklyugin, G E Norman The Moscow Physical Society, Leninskii prosp. 53, 121019 Moscow, Russian Federation. Fax (7-095)135 79 95. E-mail: gribkov@sci.fian.msk.su.

Received 26 December 1994
Uspekhi Khimii **64**(7) 643–671 (1995); translated by A K Grzybowski

approaches and the Monte Carlo method† are based on lattice models of the surface. The simpler studies are limited to the geometrical modelling of the morphology (cellular automata). In the continuous models, the surface is assumed to be a continuous function of the spatial coordinates and time. The principal problem in probability methods involves the inclusion in the latter of a universal description of the chemical bond on the surface which could be chosen for modelling the multiple repetition of elementary steps. The use of the method based on Harrison's generalised periodic system of the elements (GPSE) is very promising.[14]

The authors of the present review have confined themselves to the consideration of the simplest systems permitting modelling by the most sophisticated methods, and endeavoured to consider all the fundamental problems which determine the further development of the molecular modelling of chemical processes on the surface.

II. Classical molecular dynamics

The method of molecular dynamics (see, for example Refs 9, 15, and 16)‡ in its traditional formulation consists in the numerical solutions of Newton's classical equations for a system of N particles with a known interparticle interaction potential Φ and with specified initial conditions:

$$\frac{m_i \mathrm{d}^2 r_i}{\mathrm{d}t^2} = \nabla\Phi(r_1,...,r_N), \quad i = 1, 2, ..., N, \tag{1}$$

where m_i and $r_i(t)$ are the mass and the coordinate of the ith particle respectively. The calculated phase trajectories $\{r_i(t), v_i(t)\}$ [here $v_i(t)$ are the velocities] are used to calculate the quantities $X[r_i(t), v_i(t)]$, which depend on microscopic variables. In order to obtain the macroscopic average quantities $< X(t) >$, all these quantities are averaged either with respect to time or with respect to a set of initial states of the system. The method of molecular dynamics makes it possible to calculate the time correlation functions, the relaxation to equilibrium, etc. and also the characteristics of the equilibrium states.

Eqns (1) model a nearly microcanonical assembly (the total energy of the system remains constant on average).[7-9] In other cases, described by assemblies differing from the microcanonical assembly, the MMD equations may contain additional terms. These can represent, for example, the Langevin forces, which model the heat exchange with the external medium, or the reactions of the bonds, imposed on the system and ensuring the constancy of the thermodynamic quantities (kinetic energy, pressure) or of the spatial gradients of the macroscopic parameters (temperature, velocity).[17,18]

Depending on the problem being solved, different boundary conditions are applied to the system (periodic conditions, rigid or 'stochastic' walls, a subsystem of stationary particles, etc.).

The interaction potential Φ is frequently represented approximately by the sum of the interaction potentials of all the pairs of particles and use is made of simple analytical formulae of the Lennard-Jones, Buckingham, etc. types. The necessary number (two-three) of parameters included in them is selected on the basis of empirical data.

However, such an approach is not always applicable even to the description of the properties of condensed inert gases.[13] The situation is even more complex in the case of the atoms of other elements, between which the formation of chemical bonds, for example covalent bonds (like those between Si or Ge atoms), is possible. No pair potential ensures the stability of a tetrahedral structure of such a system because it does not give rise to even a local energy minimum for this configuration.

A somewhat different picture is observed in the case of metals.[19] With the aid of pair potentials, it is possible to describe in this instance the regular structure and energy of the equilibrium crystal. For the modelling of, for example the elastic properties, it is necessary to introduce into the total energy of the system additional terms which clearly depend on the volume of the system (i.e. which take into account the interaction of the lattice site ions through the electron gas). This approach is applicable only to 'regular' structures, where the concept of volume is unambiguously defined. For 'defective' structures (vacancies, microcracks, surfaces), the volume is not defined unambiguously and such a simple model becomes inapplicable because the dependence of the results on the volume is very marked. The problem of the formation of a chemical bond between the metal atoms and the chemically reactive impurity introduced into the metal, for example hydrogen, which was mentioned above, also remains unsolved.

Many attempts have been made to overcome the above difficulties by introducing multiparticle (ie. not reducible to the sum of pair interactions), empirical (or semiempirical) potentials.[19-35] Following the procedure of Baalamane et al.,[36] we shall divide these approaches into three main groups: the cluster potentials, cluster functionals, and inserted atom methods.

The cluster potentials[20,25,28,29,31] include the following terms, after the pair interaction terms, in the expansion of the total energy in terms of the multiplicity of the interaction:

$$\Phi = \sum_{i>j} \Phi_2(r_i, r_j) + \sum_{i>j>k} \Phi_3(r_i, r_j, r_k) + \sum_{i>j>k>l} \Phi_4(r_i, r_j, r_k, r_l) + ... \tag{2}$$

Each term represents the sum of the interaction energies $\Phi_n(r_i, r_j, ..., r_n)$ of a n-particle 'cluster', which do not reduce to a combination of the preceding terms. The series (2) usually terminates at the Φ_3 term.

Such a potential makes it possible to specify around each atom, on a sphere having a radius equal to the distance to the nearest neighbour in the crystal, four potential wells located at the vertices of a tetrahedron. This idea was first applied to the MD modelling of crystalline and liquid silicon by Stillinger and Weber (the SW potential),[20] who represented Φ as the sum of pair and three particle interactions. The pair potential has the usual form with components corresponding to attraction and repulsion and a minimum at a distance equal to the distance to the nearest neighbour in a diamond-like lattice.

$$\Phi_2(r_{ij}) = \begin{cases} A(Br_{ij}^{-p} - r_{ij}^{-q}) f_c, & r_{ij} < a, \\ 0, & r_{ij} > a, \end{cases} \tag{3a}$$

where r_{ij} is the distance between the atoms i and j and $f_c = \exp[(r_{ij} - a)^{-1}]$ is a function which smoothly cuts off the interaction at distances equal to the distance between the first and second nearest neighbours.

The three-particle potential has the form

$$\Phi_3(r_i, r_j, r_k) = h_i + h_j + h_k , \tag{3b}$$

$$h_i = \lambda \exp[\gamma (r_{ij} - a)^{-1} + \gamma (r_{ik} - a)^{-1}] \left(\cos\vartheta_{ijk} + \tfrac{1}{3}\right)^2,$$

and includes a function of the angle ϑ_{ijk} between the ij and ik bonds which in fact ensures its relative rigidity. The parameters p, q, A, B, a, λ, and γ are chosen in order to satisfy the empirical data on the structure, energy, and elastic properties of the silicon crystal.

† The Monte Carlo method, used for the molecular modelling of the structure and thermodynamic properties of equilibrium states,[12,13] has not been included in this review but is mentioned in those cases where it is employed.

‡ The importance of this method for chemical physics has been emphasised in A L Buchachenko's review [*Uspekhi Khimii* **56** 1593 (1987); *Russ. Chem. Rev.* **56** 907 (1987)].

The structure and melting point of the diamond-like silicon,[20] its phonon spectrum,[37] and even the formation of the dimers on the Si (100) surface [(2 × 1) reconstruction][38] are modelled satisfactorily with the aid of the SW potential. However, the other crystalline modifications of silicon and amorphous and liquid silicon at temperatures remote from the melting point as well as more complex reconstructions § of surfaces with different orientations are not described by potential (3).[38,39] This is not surprising, since a potential with a rigidly specified angle between the bonds does not permit the formation of a structure with a coordination of the atoms other than tetrahedral.

Nevertheless, owing to its relative simplicity, the SW potential has been used widely in calculations (see, for example, Refs 40–46). The potentials of the interaction of silicon atoms with oxygen atoms and fluorine (Si–F and Si–O) have been derived from the SW potential. They are used, for example, in the study of the chemical reactions of the silicon surface with fluorine[44,45] or of the structures and vibrational spectra of crystalline and amorphous SiO_2.[46]

The cluster functionals[18–21,23,27,29,30] have the form

$$\Phi = \sum_{i>j} \Phi_n(i,j;k \in a_n) \ . \tag{4}$$

Here each pair of interacting particles i and j in an instantaneous configuration enters into the composition of the cluster a_n comprising n particles, including those selected. The configuration of the cluster depends on the structure of the test substance (crystal, glass, etc.) and on the law governing the interparticle interaction. The energy of the interaction of a pair of particles i and j depends not only on their coordinates but also on the coordinates of all $n-2$ particles k included in the cluster a_n. The more complex form of Eqn (4) arises from the desire to construct a universal potential, i.e. to describe the greatest possible number of structures with different coordinations using a single functional form and as far as possible a single set of parameters.

The most characteristic attempt on these lines has been undertaken by Tersoff.[21–23] The main idea was to incorporate the weakening of the bonds with increase in the number of nearest neighbours of the atom participating in the formation of the bonds. The total energy of the system has the form characteristic of the pair interaction approximation.[22]

$$\Phi = \sum_{i>j} f_c(r_{ij})\left[f_A(r_{ij}) + b_{ij} f_R(r_{ij})\right] \ , \tag{5a}$$

where $f_c(r_{ij})$ is the cut-off function which determines the radius of action of the potential and $f_A(r_{ij})$ and $f_R(r_{ji})$ are the pair attraction and repulsion potentials. The coefficients b_{ij} are functions of the local environment of the particles i and j:

$$b_{ij} = \left\{1 + \beta^m \left[\sum_{k \neq i,j} f(r_{ij}, r_{ik}, \theta_{ijk})\right]^m\right\}^{-1/2m} , \tag{5b}$$

where β and m are adjustable parameters and f is a function of the coordinates of the three particles i, j, and k; the summation was carried out over all the atoms k within the radius of action of the atoms i and j. Thus the depth and position of the potential minimum for the atom i in the vicinity of the atom j depend on the instantaneous positions of all the remaining atoms of the system, which renders potential (5) in essence a multiparticle potential. This imparts to it a fairly high flexibility, which makes it possible to describe structures with different configurations when the adjustable parameters (there are 13 of these altogether) are selected successfully.

§ Reconstruction is defined as the change in the structure (and symmetry) of the near-surface layers of the crystal compared with the bulk-phase structure.

Indeed the Tersoff potential models almost all the crystalline modifications of silicon,[22] its phonon spectrum,[23] and many reconstructions of the surface.[22,37] Liquid and amorphous silicon are less successfully modelled.[23] For an appropriate parametrisation, this potential makes it possible to describe multicomponent systems[24] (which need not contain silicon), including simple chemical reactions occurring on detonation of explosives of the type $A_2 + B \rightarrow A + AB$.[47] Nevertheless, potential (5) is not fully universal, since for the calculation of different properties and structures it requires different parametrisations.[22,23] For example, when the parameters of Eqn (5) are selected for the best description of the dependence of the energy on the specific volumes of different crystalline modifications of silicon, the accuracy of the calculation of the phonon spectrum is lost, and conversely.

The inserted atom method (IAM).[19] The total energy of the system assumes the form

$$\Phi = \sum_{i>j} \Phi_2(r_i, r_j) + \sum_i F(\rho_i) \ , \tag{6}$$

where Φ_2 is the energy of the pair interaction of ionic cores, $F(\rho_i)$ is the energy of the atom i 'inserted' in a medium having at the site of insertion an electron density ρ_i, which is generated by the electrons of all the remaining atoms of the system and is assumed to be additive, i.e.

$$\rho_i = \sum_{j \neq i} \rho(r_{ij}) \ , \tag{7}$$

$\rho(r)$ being the density of the electrons in the atom of the test element at a distance r from the nucleus. The last function is determined either from quantum-mechanical calculations or from empirical data. The functions Φ_{ij} and $F(\rho)$ in the initial formulation of the inserted atom method were selected by adjustment for consistency with empirical data for the crystal (the lattice constant, the elastic constants, the sublimation energies of various crystalline modifications, the formation energy of a vacancy).

It is seen from Eqns (6) and (7) that there is a relation between the IAM and the method of cluster potentials. Thus, if the function $F(\rho)$ is linear, then the IAM is equivalent to the approximation of pair interaction potentials, since the force acting on the atom i is proportional to the sum of functions which depend only on r_{ij}. For a quadratic variation of $F(\rho)$, we arrive at the triple potentials approximation, etc. This approach has been assigned[36] to the method of cluster functionals. We segregated it in a separate group because different physical considerations are employed in constructing the right-hand sides of Eqns (4) and (6). This is associated with the fact that initially these two methods developed in relation to different groups of elements: to Group IV semiconductors and metals respectively.

The relation[34]

$$F(\rho) = -c\rho^{-1/2},$$

which is universal for all metals, has been largely used recently for $F(\rho)$. This is based on the possibility of interpreting $\rho(r)$ in Eqn (7) as the square of the overlap integral of the wave functions of the atoms i and j.

The IAM has been applied successfully to the study of the structures and diverse properties of metals and alloys (including liquid ones): defects, the structures of the surfaces, various reconstructions, the phase structures of alloys, the bulk-phase and surface phonons, the structures of the interfaces, and the hydrogen on the surface (see, for example, Baskes et al.[35] and the references quoted therein).

The attempt to extend the IAM to systems with covalent bonds (Si and Ge)[35] has not been very successful. In particular, it leads to the 'external relaxation' of the surfaces on

reconstruction, i.e. the distance between neighbouring crystalline planes increases near the surface and does not diminish as would be expected from experimental data and which has been confirmed by other theoretical models. The IAM method[35] has been extended[48] to 26 elements (mainly metals). Certain deficiencies of the potentials[35] have been corrected, but a radical improvement could not be achieved for silicon and germanium.

III. The regions of applicability of the adiabatic approximation

As early as 1988, Tersoff,[22] who proposed one of the most successful cluster functionals, expressed doubts concerning the possibility of constructing a fully universal empirical potential. Having compared the results obtained with the aid of six potentials from different groups, the authors of a critical review[36] concluded that they are not universal and that no potential has decisive advantages which would lead to its being preferred to others. It was concluded that a universal potential cannot be constructed.

The causes of the relative failure of the group of methods employing the interaction potentials of the particles in calculations of their motion (the potential approach) have been specified as "...the general inability to model the formation of π-bonds" and "...the inadequacy of the description of angular forces", i.e. there is a direct indication that many quantum-mechanical effects cannot be described with the aid of classical potentials.

We shall now consider the limits of the applicability of approximation (1).

The use of the potential Φ is valid only in terms of the adiabatic approximation. In this case, the potential $\Phi(R_i)$ is a solution of the problem of the determination of the eigenvalue of the equation

$$\left(-\frac{\hbar^2}{2m}\sum_{i=1}^{n}\nabla_i^2 + V(R,r)\right)\varphi_R(r) = \Phi(R)\,\varphi_R(r)\ , \qquad (8)$$

where the summation is carried out over all the electrons. The term ∇_i denotes differentiation with respect to the electronic coordinates r_i and V denotes the interaction of all the charges [R and r are the sets of coordinates of the ions and electrons and $\varphi_R(r)$ is the wave function of the electron subsystem, which depends parametrically on the ionic coordinates R].[99]

The wave function in Eqn (8) refers to a specific state of the electron. For example, the ground state of crystalline silicon corresponds to the diamond lattice and is described by the wave function φ_0, which represents a linear combination of the sp^3 orbitals for each atom. The potential curve *1* in Fig. 1*a* corresponds to this structure. Another wave function and hence another potential curve (curve *2*) correspond to any metastable crystalline modification of silicon (for example, the simple cubic modification). We may note that, depending on the average distances between the ions, the ground states of the lattice may prove to be the states of structures of different symmetries. Strictly speaking, different structures should be modelled by different potentials.

Nevertheless, with the aid of the same empirical classical potential, it is possible to model not only the global but also certain local energy minima in the configuration space. The explanation for this is that the potentials examined in Section II do not follow from Eqn (8). They contain a large number of adjustable parameters, the successful selection of which permits the construction of a potential surface similar to that illustrated by a dashed line in Fig. 1*a*.

In order to understand the possibilities and limitations of this approach, it is necessary to apply Massey's adiabaticity criterion:[5,99]

$$\frac{a\Delta\Phi}{\hbar v} \gg 1, \qquad (9)$$

where a is the characteristic distance over which $\varphi_R(r)$varies, $\Delta\Phi$ the distance between the adiabatic potential surfaces, and v the characteristic velocity of the heavy particles. Thus the adiabatic approximation is valid over the entire range of values of R, except in the regions of the intersections (or the pseudo-intersections) of the adiabatic potential surfaces.

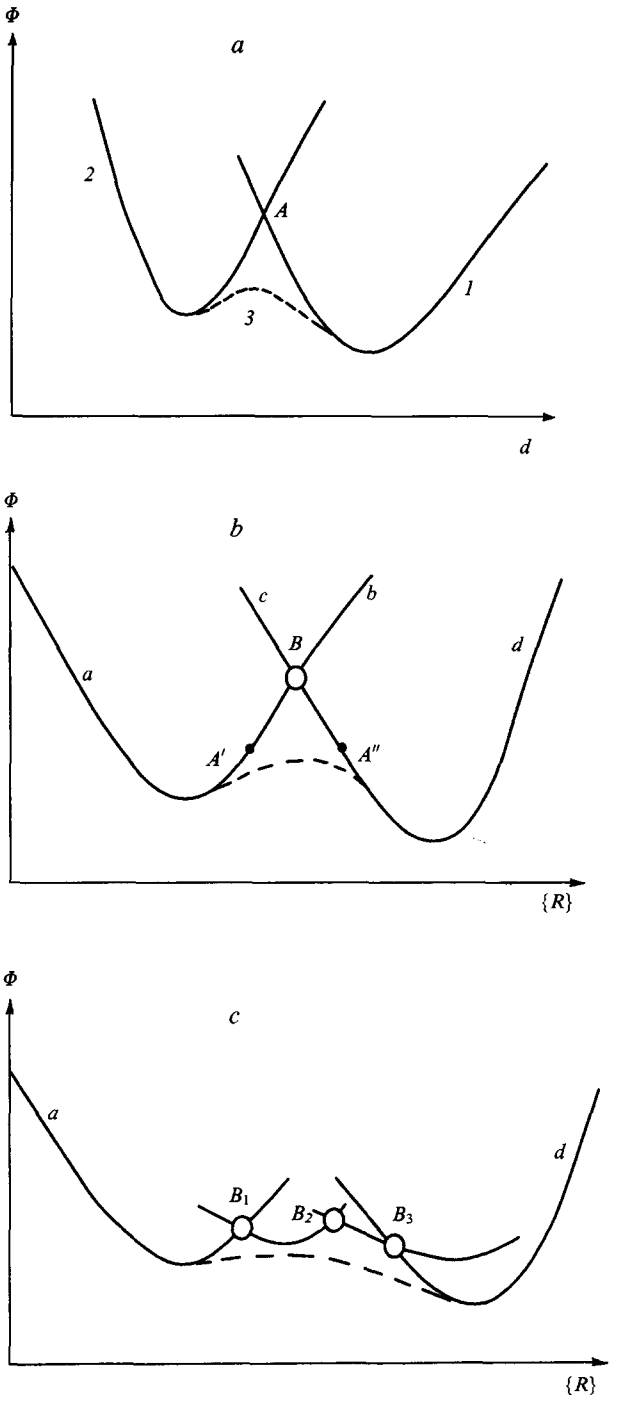


Figure 1. Conventional schematic illustration of adiabatic potential surfaces and nonadiabaticity regions: (*a*) potential curves for different regular crystalline structures as a function of the distance (d) to the nearest neighbour: continuous lines *1* and *2*—exact quantum-mechanical calculation, dashed line *3*—model potentials; (*b*) potential surfaces in the configuration space; the circle B represents the region of nonadiabaticity; (*c*) schematic illustration of numerous potential surfaces.

In the vicinity of such intersections, the motion of ions may induce nonadiabatic electronic transitions, the representation of the wave function for the system in the form of the product of the electronic anionic components becomes impossible, and approximation (8) loses its physical significance. The solution of

the dynamic problem in this (nonadiabatic) case must involve the study of electronic transitions.

In other words, the adiabatic approximation is by no means valid over the entire range of the possible values of R for a polyatomic system and the use of Eqns (1) with $\Phi(R)$ is possible only in the regions of the configuration space R (hypervolumes) separated from one another by hyperlayers, where approximation (1) is in principle impossible. The thickness of such layers may be estimated with the aid of Eqn (9).

Fig 1*a* does not illustrate this situation, since the point A does not correspond to the intersection of the surfaces $\Phi(R)$ in the space $\{R\}$ (Fig. 1*b*). The points A' and A'' in Fig. 1*b* correspond to identical distances to the nearest neighbour, i.e. to the point A in Fig. 1*a*, but they are completely different points in the configuration space. The potential surface for the ground state (the aBd curve) is divided into the adiabatic regions $aA'B$ and $BA''d$ corresponding to different electronic states (which in turn correspond to different symmetries), the adiabatic approximation breaking down in the vicinity of the boundary between them (the region of the point B).

Fig. 1*b* illustrates highly schematically the principal idea, although it does not in fact correspond to reality — the potential surfaces for the diamond and simple cubic lattices in the configuration space cannot intersect anywhere. Any path in this space, connecting the points corresponding to these structures, passes in succession through the points B_i at which there are intersections with the potential surfaces of the excited states (there are only three such points in Fig. 1*c*). The degeneracy of these points can be removed by taking into account any of the interactions disregarded previously, but in this case Massey's criterion necessitates a quantum treatment of the region B_i, although this is not in fact important.

The motion of the atoms within the adiabatic regions (aB and Bd in Fig. 1*b* and aB_1, B_1B_2, B_2B_3, and B_3d in Fig. 1*c*) obeys Eqns (1). On the other hand, when the regions intersect at the points B_i, Eqns (1) lose their significance — the potential $\Phi(R)$ cannot describe the interaction of heavy particles. Electronic transitions may occur in these regions and the trajectories may undergo branching. The choice of the type of extension of the trajectories must be made with the aid of statistical modelling based on the quantum-mechanical calculation of the amplitudes of the transition probabilities. Such an approach is valid if the nonadiabatic regions B_i in the phase space are much smaller than the regions corresponding to classical motion. In this section, we shall confine ourselves to the consideration of the quantum effects associated with the interaction and will not be concerned with cases where the de Broglie wavelength of the heavy particles becomes comparable to a and interference effects appear.

Thus the empirical potentials (the dashed lines in Figs. 1*a* – 1*c*) may describe the properties (including the time correlations) of the stationary state of the system in the vicinity of several (but not all!) local minima. However, the transitions between these states, obtained by the MMD, are not transitions with a real dynamic process occurring in the course of the correct time. For this reason, the processes accompanied by electronic transitions, for example the kinetics and times of the reconstruction of surfaces, are difficult to describe with the aid of the MMD in its classical formulation.

Example. We shall analyse a study[42] in which the temperature dependence of the velocity of the phase transition front (solidification or fusion) in silicon was investigated with the aid of the SW potential. The calculation was performed as follows. A rectangular parallelepiped was examined; 24 crystal planes, containing 18 silicon atoms each, passed through it parallel to its bases. Periodic boundary conditions were applied in the directions parallel to the planes. The atoms in two planes closest to one of the bases are stationary and occupy the crystal lattice sites. The atoms in the third and fourth layers are used to supply or remove heat (a constant temperature is maintained for these atoms with the aid of a scaling recalculation of the velocities). The remaining atoms of the system obey the usual MD [Eqns (1)] and are referred to as MD atoms.

In the initial instant, the MD atoms are either in positions corresponding to a specially prepared melt (in the modelling of crystallisation) or at the crystal lattice sites (in the modelling of fusion). The distribution of the velocities of these atoms corresponds to a certain initial temperature. The required phase transition temperature is then specified for the atoms of the third and fourth layers and is subsequently maintained constant. The heat exchange front gradually spreads towards the MD layers and leads to a structural rearrangement of the atoms (the phase transition).

Any layer is regarded as having become crystallised when its particles have become stably localised in the vicinity of lattice sites. Conversely, a layer is regarded as having fused when the particles have moved away from the vicinity of the lattice sites.

The results of the calculation are compared with experimental data in Fig. 2, which also presents the curves for the classical transition state theory. We may draw attention to a significant scatter, increasing on passing to fusion [$V(T) < 0$], which indicates a less satisfactory description of the fusion process. From our point of view, this scatter does not reduce to a statistical scatter but can be accounted for by the following causes:

On crystallisation, the particles 'roll down' into the potential well, the depth and position of which are determined beforehand by the particles of the preceding, already 'solidified', layers. In this case, the process activation energy is low (if it exists at all) and the results of the classical and quantum calculations may be similar.

On the other hand, on fusion such potential wells are not prepared beforehand. The atoms must 'collectively' seek the energy minimum. Such a process may be accompanied by the overcoming of high potential barriers, as a result of which the system may be fixed at local (metastable) minima, with which the scatter of the results may in fact be associated. In this case, the results of the classical and quantum-mechanical calculations will not agree and the possibility of determining the velocity of the fusion front within the framework of the adiabatic approximation (1) is open to doubt. The discussion of these questions will be continued in Sections IV, V, and VI.

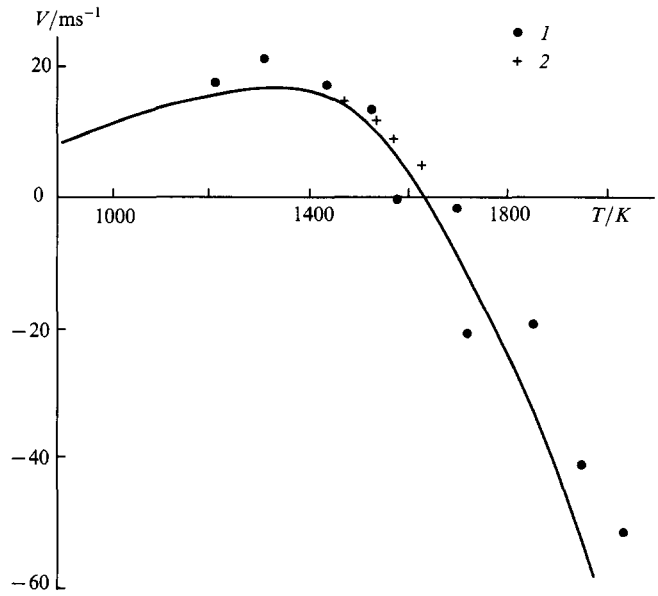


Figure 2. Temperature dependence of the velocity of the phase transition front. The positive velocities correspond to hardening and the negative ones to fusion. The curve was obtained by means of the transition state theory: (*1*) calculation; (*2*) experiment.

IV. Adiabatic quantum molecular dynamics

Approaches, which are frequently referred to as quantum MD, have developed in recent years in parallel with the potential approach. The scheme of Car and Parrinello (CP)[49] and the tight-binding method,[50,51] genetically related to the first procedure, are the most popular and will be briefly discussed in this Section.

1. The method of Car and Parrinello

The CP method involves the simultaneous calculation of the dynamics of valence electrons and ions (ionic cores),[52] the ions being considered in terms of the classical approximation and the electrons in terms of the quantum-mechanical approximation. Suppose we have a system of N ions with a mass M, described by the coordinates R_i ($i = 1, \ldots, N$) and the velocities $\dot{R}_i$, and N_1 electrons in the ground state and characterised by a set of wave functions (orbitals) $\psi_j(t)$ ($j = 1, \ldots N_1$). The latter may be expanded in terms of a set of basis functions $\chi_1, \ldots \chi_m$.

$$\psi_j(t) = \sum_k C_k^j(t)\chi_k .$$

The significance of coordinates and velocities of the electron subsystem is attributed to the amplitudes C_k^j and their derivatives with respect to time $\dot{C}_k^j$. Thus if the dependence of the potential energy E_{tot} of the system on R_i and C_k^j is known, it is possible to construct the pseudo-Lagrangian

$$L = \frac{\mu}{2}\sum_j\sum_k(\dot{C}_k^j)^2 + \frac{M}{2}\sum_k\dot{R}_i^2 - E_{tot}(C_k^j, R_i) .$$

Here the first term is the fictitious kinetic energy of the electronic component and μ the fictitious mass of the electron, the choice of which will be discussed below. Having supplemented the pseudo-Lagrangian by the condition that the functions ψ_j are orthonormalised

$$\sum_k C_k^{j*}C_k^j - \delta_{ij} = 0, \tag{10}$$

it is possible to obtain the equations of motion of the electrons and ions.

$$\mu\ddot{C}_k^j = -\frac{\partial E_{tot}}{\partial C_k^j} - \sum_l \lambda_{jl}C_k^l, \tag{11a}$$

$$M\ddot{R}_i = -\frac{\partial E_{tot}}{\partial R_i} . \tag{11b}$$

The last term in Eqn (11a) represents the response to the 'binding' [Eqn (10)] and λ_{jl} are undefined Lagrange multipliers, which are found simultaneously with the solution of Eqns (11).

The energy of the system E_{tot} is determined by the density functional method (see, for example, Yin and Cohen[53]). A system of planar waves is generally chosen as the basis system. Eqns (11) are solved numerically by methods analogous to those employed for the integration of classical MD equations. The scheme used in the solution, the minimisation of the initial electron energy (the adjustment of the energy of the electron subsystem to the Born–Oppenheimer surface, i.e. to the ground state) for fixed initial positions of the ions, the choice of the number of basis functions, etc. have been discussed in detail in a review.[52]

The theoretical justification of the CP method[49] consists in the fact that the solution of Eqns (11) under conditions where the trajectories reach equilibrium and in the temperature limit $T \to 0$ ('annealing') makes it possible to find the states of the electron and ion system (wave functions and coordinates) which gives rise to a minimum in the density functional. The $T \to 0$ annealing procedure is an important element of the CP method.

The principal difficulty in the application of the CP method (the maintenance of the constancy of the overall kinetic energy of the ions and E_{tot} at finite temperatures) is associated with the presence of the fictitious kinetic energy of the electrons, which depends on the fictitious mass μ. In choosing μ, it is necessary to seek a compromise. On the one hand, in order to diminish the oscillations in the 'real' energy, μ must be reduced. On the other hand, μ determines the minimum permissible time step in the integration and, in order to decrease the computational time, it is desirable to increase μ. This question as well as other procedures for the attainment of adiabatic conditions have been examined in a number of studies.[52,54,55]

The CP method has been applied successfully in the calculation of the structures (including the electronic structure) and properties of systems such as the protons in crystalline silicon,[56] liquid and amorphous silicon[54,57,58] and carbon,[59,60] liquid metals,[61] crystalline ice,[62] and liquid water.[63]

The fundamental limitation of the CP method in its current formulation is that the electrons exists only in the ground state, i.e. are on the Born–Oppenheimer surface, which is different for different characteristic structures (crystalline, liquid, and amorphous). Being capable of describing each of these structures, the CP method is not in principle designed to calculate the transitions between them. In this respect, the CP method is even more limited than the potential approach.

Thus, by resorting to CP quantum dynamics, we cannot solve the problem of the description of transitions between different electronic states.

The CP method proved to be extremely powerful, but it requires an enormous expenditure of computer time. This is associated with the simultaneous numerical integration of the equations of motion of the ions and electrons. The small time step in the integration is determined by the low fictitious mass of the electron, but the overall time is determined by the characteristic times of the dynamics of the ions. The total number of steps proved to be very large. The second cause is the enormous number of planar waves necessary for the calculation (several hundreds for semiconductors and several thousands for metals).

These factors limit the number of atoms involved in the calculation to ~ 100, whereas the number of particles required in calculations for complex reconstructions, dislocations, and real surfaces is much greater.

2. The tight-binding method

The wish to reduce the requirements for computer resources associated with the CP method led to the appearance of its simplified versions — the so called tight-binding methods (TBM). These methods make it possible to accelerate the computations by factors of tens and hundreds at the expense of accuracy.

In the most radical version[50] of the TBM, the following principal simplifications, compared with the CP scheme, are introduced:

(a) The abandonment of the explicit calculation of the electron dynamics.

(b) The choice as basis functions of only a small number of valence electron orbitals in the consideration of the crystal structure (four sp^3 orbitals per atom for diamond-like Si).

(c) The forces F_i acting on the ions from the electrons are calculated in accordance with the Hellmann–Feynman theorem

$$F_i = \sum_j < \psi_j|\frac{\partial \hat{H}}{\partial R_i}|\psi_j > ,$$

where $\hat{H}$ is the Hamiltonian of the electron subsystem (the summation is carried out over all occupied electronic levels).

(d) Interionic pair potentials are introduced in accordance with the equation

$$\Phi_2(R) = E_{tot}(R) - E_{BS}(R) , \tag{12}$$

where E_{tot} is the total potential energy of the system determined by the density functional method[64] and E_{BS} is the energy of the band structure calculated in accordance with the tight-binding empirical scheme.[65] The quantities $E_{tot}(R)$ and $E_{BS}(R)$ are found for a regular crystal structure per atom of the crystal.

Thus the equations of motion of the ions assume the form

$$M\ddot{R}_i = F_i - \nabla_i \sum_j \Phi_{ij}.$$

They are solved according to the following scheme: (1) adjustment of the energy of the electrons to the Born – Oppenheimer surface for the initial positions of the ions; (2) calculation of the forces F_i; (3) calculation of a single time step for the ions; (4) recalculation of the wave functions and return to step 2.

The phonon spectra of diamond-like silicon,[50] the fine anharmonicity effects (thermal expansion, the shift and broadening of the phonon lines with increase in temperature) in diamond-like silicon,[66] the degree of adsorption of hydrogen on the (100) surface of diamond,[67] etc. have been calculated with the aid of the TBM.

The attempts to apply the TBM to the modelling of different Si and Ge surfaces demonstrated its nonuniversality,[68] analogous to the nonuniversality of the classical potential approach. The reason for this is that a system of basis wave functions specific to a tetrahedral structure is employed. This system is unsuitable for the description of electronic structures with symmetries other than tetrahedral, which have other wave functions.

These considerations led Mercer and Chou[68] to the conclusion that the TBM must be parametrised for Si and Ge. Here $E_{BS}(R)$ is again calculated for the sp^3 orbitals, while $E_{tot}(R)$ is calculated separately for each of the large number of crystalline modifications. Thus the interionic pair potential $\Phi_2(R)$ is found to be different for different crystal lattices, i.e. its dependence on the coordination appears. This dependence was in fact parametrised in such a way that $\Phi_2(R)$ was a function of the local environment of the given atom, i.e. of the local coordination number. This procedure is fully analogous to that employed by Tersoff[22] in the classical potential approach. In this approach, $\Phi_2(R)$ is a cluster functional.

The parametrised TBM is extremely flexible, i.e. it makes it possible to describe successfully virtually all reconstructions of the Si or Ge surfaces with the aid of the same (for each element) set of adjustable parameters.[69]

Thus the situation illustrated schematically in Fig. 1 is also repeated in the TBM. By using this method, it is possible to construct a potential surface having local minima close to the real minima for different electronic states (terms). On the other hand, it is clear that the dynamics of the transitions between these states cannot be reproduced by such procedures. The CP and TBM methods operate only with stationary solutions of the Schrödinger equation. On the other hand, the description of the electronic transitions requires the solution of nonstationary quantum-mechanical equations.

V. Reconstruction, adsorption, surface diffusion, clusters

1. Modelling of the surface

The block of mobile particles in the MMD is referred to as the basic cell (BC). For the surface of a crystal, it consists of a certain number of layers of particles and is bounded 'from below' by a layer (or several layers) of stationary particles. When necessary, the deeper layers can be replaced by a continuous medium, which acts on the BC in accordance with the Mie or Steele potentials.[6] We select a cell with a height h and a length and width l [in the horizontal directions, the BC is either also bounded by layers of stationary particles or periodic boundary conditions (PBC) are used in these directions]. The number of particles in the BC is $N = nl^2h$, where n is the average concentration of particles.

The choice of the dimensions of the cell. Modelling a section of the surface, is made in such a way that the motion of individual atoms reproduces characteristics of the phonon spectrum important for the given problem; the reconstruction and relaxation of the cell surface are reproduced.

In the modelling of equilibrium processes (desorption, surface diffusion, incidence of thermal particles) at a certain temperature, the size of the cell is chosen on the basis of the conditions l, $h > k_{min}^{-1}$, where k_{min} is the minimum wave vector of the phonons which still contribute to the energetics of the process investigated.

In the modelling of nonequilibrium processes (incidence of fast particles), the size of the BC must be chosen so that the interaction time t_1 (the computation time) is much shorter than the time t_2 required for the return to the surface of the nonequilibrium excitation reflected from the BC boundary:

$$t_1 \sim \frac{\sigma}{v_{inc}} \ll t_2 \sim \frac{l}{c} \left(\text{or } \frac{h}{c}\right), \tag{13}$$

where σ is the characteristic dimension of the potential, v_{inc} is the velocity of the incident particle, and c the speed of sound.

There exists a procedure for softening condition (13) by introducing the removal of heat into the calculation. The Langevin terms (the δ-correlated random force and friction linked in accordance with the fluctuation-dissipation theorem) are then introduced into the equations of motion (1) for the boundary particles in the BC. They model thermal conduction, quenching the nonequilibrium excitations arriving at the cell boundary. The inequality (13) is replaced by the condition $t_1 < t_2$.

The above conditions are useful for the estimation of the characteristic dimensions, because the quantities involved in them are frequently known only in terms of order of magnitude. It is desirable that the choice of the final BC dimensions (and boundary conditions) should be made on the basis of the results of trial calculations.

Boundary conditions. The reconstruction and relaxation of the surface can be modelled only with the aid of PBC. On the other hand, if the structure of the surface is already known, then the corresponding geometry can be specified for a bounded cell. Nevertheless it appears that an equal degree of uniformity of the BC along the horizontal plane is attained for PBC when the BC size is smaller than for a bounded cell.

The removal of heat is more naturally modelled for a bounded BC, because it can be achieved in all directions, whereas for PBC it is possible only in the 'downward' direction. The reproduction of the removal of heat for PBC requires an increase in the size of the BC compared with the bounded cell.

Averaging. The result of the interaction of an incident particle with the surface depends on the position of the target point relative to the surface atoms. Therefore, if interaction coefficients averaged with respect to the surface are required, the averaging must be carried out with respect to all the positions of the target point within the limits of the projection of the unit cell of the crystal (or the BC for a noncrystalline body) on the surface. Naturally, for a reconstructed surface the averaging region is greater than for a nonreconstructed surface. The statistical error increases owing to the motion of the surface atoms, which in fact never occupy equilibrium positions.

2. Reconstruction

Flat surface. An attempt at the classical modelling of the dynamics of the initial stage of the reconstruction (dimerisation) of the Si(100) and Ge(100) surfaces and of their equilibrium struc-ture has been undertaken[70] with the aid of potentials of the SW type.

In the initial instant, all the atoms occupy the sites of a tetrahedral structure and have velocities with a Maxwellian

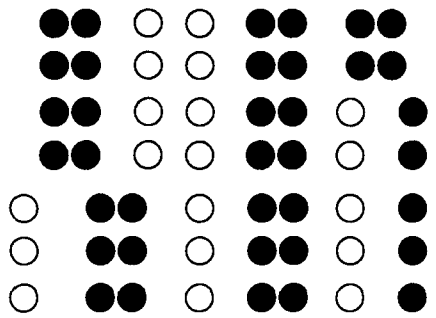


Figure 3. Schematic illustration of the first layer of a reconstructed silicon surface.

distribution at the temperature considered. In the course of the computation, the nonequilibrium initial structure evolves to a reconstructed structure containing ordered rows of dimers (Fig. 3). The reconstruction takes place as follows: the formation of a dimer at any surface site induces the rapid dimerisation of two adjoining atoms, etc., i.e. a growing row of dimers appears. Two rows of dimers, growing in opposite directions, can meet and form a single long row. If the rows are displaced relative to one another when they meet, then 'free' atoms are formed at the meeting point.

The properties of the equilibrium structure obtained correspond to the available experimental data. The average distance between the atoms in the dimer proved to be 2.42 Å (the experimental values range from 2.36 to 2.47 Å). The qualitative explanation of the experimentally observed transition from the $c(4 \times 2)$ structures (inclined asymmetric dimers) and $p(2 \times 2)$ structures (inclined symmetrical dimers) at low temperatures to structures with the (2×1) symmetry (noninclined dimers) at high temperatures is one of the most interesting results.[70] From the standpoint of the MD experiment at finite temperatures, the inclined dimers are always present owing to the thermal shift, i.e. the 'instantaneous photograph' always reveals their presence. However, at low temperatures the slopes of neighbouring dimers are correlated — they exist in the counterphase. This in fact yields an instantaneous picture of type $c(4 \times 2)$ reconstructions. Owing to the intensification of thermal motion, at high temperatures the inclinations of the dimers become noncorrelated, which corresponds (on average) to the (2×1) symmetry.

The attempt to apply the more complex Tersoff potential showed that the latter yields a force of attraction between the atoms in the dimer which is too large (Fig. 4).

Calculations have also been made[70] of the reconstruction times, but these results may be open to doubt (see Section III).

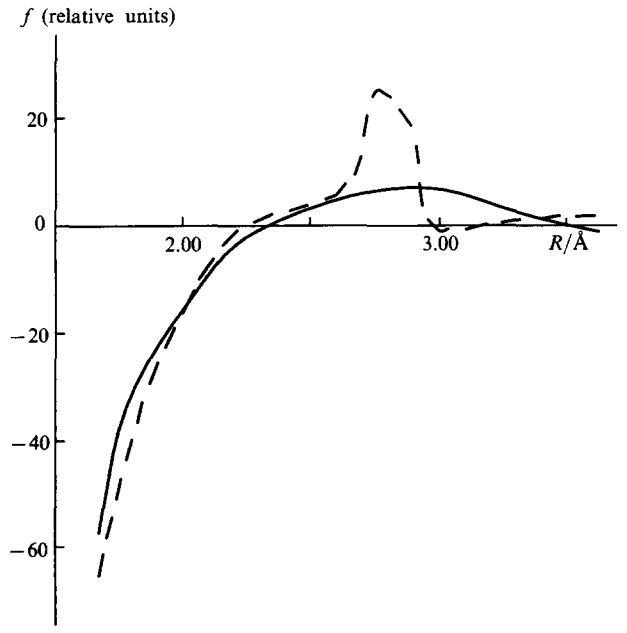


Figure 4. Forces acting in the direction between the atoms in the dimer for different potentials. Continuous line — calculation employing the SW potential; dashed line — calculation employing the Tersoff potential.

Steps. In a study of the atomic and molecular structures of monomolecular steps on the Si(001)−(2 × 1) surface, the Car–Parrinello method was employed.[71] A cell comprising seven layers was considered. The free bonds of the lower layer of silicon atoms were saturated by 48 oxygen atoms.

For a flat surface, it was found that symmetrical dimers, i.e. those in which both atoms have the same coordinate z, are unstable. Compared with $s(2 \times 1)$, the $b(2 \times 1)$ reconstruction (inclined dimers in which the difference between the levels of the atoms is $\Delta z = 0.51$ Å) lowers the overall energy by 0.10 eV dimer^{-1}. The ground state of a flat surface proved to be the $c(2 \times 4)$ reconstruction (the directions of inclination of neighbouring dimers in one row and on passing from one row to another alternate, $\Delta z = 0.72$ Å, and the decrease in energy is 0.24 eV dimer^{-1}). The $p(2 \times 2)$ reconstruction with $\Delta z = 0.72$ Å is inferior to the latter only to the extent of 8 meV dimer^{-1}.

The geometry of a monomolecular step may be extremely varied. Fig. 5 illustrates three configurations: S_A — the upper terrace dimers perpendicular to the edge of the step (Fig. 5*a*), S_B — dimers parallel to the edge of the step whereupon the step may be terminated by the row of atoms of the lower terrace, the corresponding dimer pair which is ahead of the upper terrace (Fig. 5*b*) or under it (Fig. 5*c*) (the nonrebonded and rebonded edges). The combination of the inclinations of the dimers, the

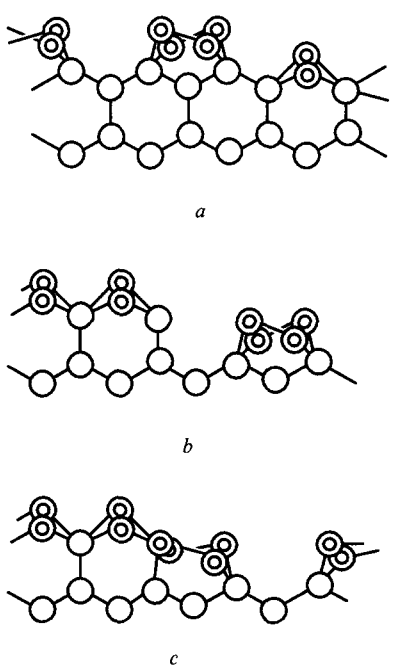


Figure 5. Schematic illustration of a step on the surface of silicon for three configurations: (*a*) S_A; (*b*) S_B (nonrebonded edge); (*c*) S_B (rebonded edge). The double circles denote the atoms of surface dimers. Apart from the atoms of the dimers, which are in the plane of the figure, the atoms in the next plane (in depth) are also shown.

different reconstructions of the upper and lower terraces, and the edges of the step decrease by a large factor the number of possible configurations. Boguslawski et al.[71] modelled only eight principal cases, including those variants of the S_A and S_B steps which had been observed experimentally.

Calculation of the electron dynamics enabled the authors[71] to reproduce the specimens observed in a scanning tunnel microscope and to compare them with the results of measurements. The qualitative features of experimental data could be explained on the basis of the shape of the wave functions of the surface states without additional hypotheses concerning the reconstruction induced by the blade.

3. Sticking, accommodation, adsorption, and scattering

The elementary sticking and accommodation steps have been widely investigated by the MMD, for example in Refs 41 and 72–74. We shall consider the study[41] where the sticking and energy accommodation coefficients for the atoms X (helium, neon, and argon) on falling on the Si(100) surface were calculated in the range of energies of the incident particles from 0.1 to 1 eV and at surface temperatures from 300 to 1000K. The Si–Si interaction was described in terms of the SW potential. The interaction of the X atoms with the Si atoms was described with the aid of the Lennard–Jones potentials.

The X atoms were projected towards the surface and at right angles to it from a certain distance z_0, selected at random, over which the X–Si interaction is virtually nonexistent. The initial position of the atom relative to the region of mobile surface particles was also selected at random. The distribution of the initial velocities of the moving surface particles was of the Maxwellian type at a temperature T_s in the range from 300 to 1200 K. The trajectories of all moving particles were calculated.

A particle was regarded as having been reflected when the condition $z > z_0$ (z being the current distance between the atom and the surface) was fulfilled, i.e. if the particle intersected the plane of projection in the opposite direction. This criterion of reflection leads to prolonged calculations, but it is necessary for the accurate calculation of the energy accommodation coefficient.

The atom is regarded as sticking if the direction of its velocity changes four times. Sometimes the first return of the particle to the surface is regarded in the literature as sticking.[74] However, visualisation of the calculations shows that the particle is in many cases reflected after the second collision with the surface atoms. On the other hand, instances of reflection after the third collision during the residence time of the X particles within the confines of the modelled block have not been observed.

After the completion of the calculation in each attempt, the surface particles return to the initial position with a new Maxwellian velocity distribution. The total number of attempts N for each energy E_i was 100. The sticking coefficient k_{st} is defined as the ratio of the number of attempts with sticking M_{st} to the total number of attempts M.

Fig. 6 presents the results of the MD calculations of the coefficients of sticking to the nonreconstructed Si (100) surface. The sticking coefficients diminish with decrease in the mass of the incident particles, with increase in their energy, and also after an increase in the temperature of the surface. A procedure has been proposed[41] for reconciling the results of the calculation with the analytical rigid cubes model[75] by introducing into the latter an effective angle of incidence ϑ.

A dependence on the mass of the incident particles is manifested also in interaction with the surfaces of polymers; we shall return to this question at the end of this section.

Methods in which the sticking of a gas to the surface is considered within the framework of the approximation where the incident atom is classical (quasi-classical) but the phonons are treated quantum-mechanically have been analysed.[76] A model example of the sticking of He, Ne, and Ar atoms to the surface of copper has been quoted.

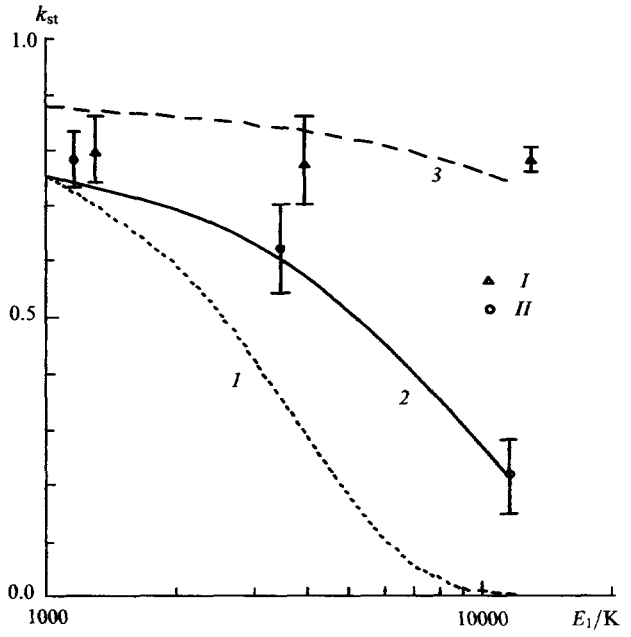


Figure 6. Dependence of the sticking coefficient on the energy of the incident particle. MD calculation: (*I*) Ne, surface temperature T_s = 640 K; (*II*) He, T_s = 1160 K. Rigid cubes model: (*1*) He (angle of incidence $\vartheta = 0$); (*2*) He ($\vartheta = \pi/6$); (*3*) Ne ($\vartheta = 0$).

The enthalpies of adsorption of 13 hydrocarbons (pentane, cyclohexane, 2-methylbutane, decane, etc.) on a mineral smectic clay have been calculated with the aid of the classical MMD.[77] The significant sensitivity of the results to the choice of the parameters of the Lennard–Jones potential used for the description of the interaction of the nonbonded atoms with one another was elucidated. None of the sets of potentials known in the literature made it possible to achieve agreement with experimental data.

Various equilibrium states of hydrogen adsorbed on the (001) surface of diamond have been considered by the tight binding method.[67] The method of molecular dynamics has been used only in the gradient descent method, i.e. as a procedure for the fastest determination of the location of the energy minimum for a system which was initially close to the configuration of the system under consideration. The structures of the clean C(001) surface and two structures with adsorbed hydrogen — monohydrogenated (001) — (2 × 1) : H (phase *1*) and dihydrogenated (001) — (1 × 1) : H (phase *2*). The structures of the electron bands and the density of the electronic states were calculated. It was found that there are no electronic states in the forbidden band gap in phase *2*, while in phase *1* they do exist. Yet another qualitatively explained effect is the repulsion of the surface electronic states in phase *2* into the conduction and valence bands. In the latter case, the surface electronic state is in resonance interaction with the electronic level of the C atom, which actually leads to an increase in the conductivity of diamond by several orders of magnitude after its treatment in a hydrogen atmosphere. This effect is apparently of a purely surface type.

For high energies of the incident particles, the treatment is restricted to the simplest interaction potentials. The individual trajectories of the incident Ne^+ ion (2 and 4 keV)[78] were modelled by a sequence of pair collisions with surface atoms. Account was taken of the collective effects when the Ne^+ ion interacts almost simultaneously with a group of atoms arranged in a nearly symmetrical configuration around the trajectory of the ion (chanelling is a typical example).

The scattering of ions on different Ni faces on the reconstructed Pt(110) – (1 × 2) and – (1 × 3) surfaces as well

as the dislodgement of the oxygen atoms adsorbed on Ni were investigated. The results agree satisfactorily with experiment.

4. Surface diffusion

The diffusion of rhodium and nickel adsorbed atoms on the (111) and (001) surfaces of rhodium and nickel respectively has been considered.[79] The Morse and inserted atom potentials were used. The distributions with respect to energies and the relation between the rotational and translational energies in the diffusion of a CO molecule on the Ni(111) surface have been determined in another study.[80] Tully's stochastic dynamics was used. The non-Arrhenius temperature dependence of the calculated diffusion coefficients is noteworthy. A comparison was made with Kramers theory.

Wang et al.[81] carried out calculations for the diffusion of a CO molecule on the Pt(111) surface at temperatures in the range 100–500 K. The surface was specified by a potential which depends on the coordinates of the stationary platinum atoms. The CO molecule was oriented mainly at right angles to the surface. The dependence of the diffusion on the rotational and vibrational states of CO was noted. The diffusion coefficients obtained agreed with the available experimental data within the limits of the scatter of the latter. An attempt was made to model the energy exchange between CO and the surface by including the interactions of the molecule with phonons. In view of the increase in the required computation time by a factor of 100, only two trajectories were calculated. They showed that the energy exchange influences the diffusion.

Engdahl and Wahnström[82] investigated the nonequilibrium diffusion of hyperthermal adsorbed oxygen atoms arising on dissociative chemisorption of the O_2 molecule on the Al(111) surface. In view of its complexity, the chemisorption process was not considered. The initial condition chosen was such that the bond in the O_2 molecule had already been ruptured and the atoms had moved apart so much that the interaction had been neglected. The initial energies of the O atoms were chosen to be 3.5 eV, which corresponds to the energy of the chemisorption of O atoms, and 9.5 eV (for comparison). The inserted atom potentials and Tulley's model were employed. In the model, the Langevin equations were used for the atoms of the third layer, while the atoms of the fourth and deeper layers were fixed in the equilibrium positions.

It was shown that the atoms are mainly displaced in the ballistic stage over a period less than 0.5 ns. Further thermalisation requires a longer time (> 5 ns) but takes place without a directional shift. The ballistic shift is 16 Å for an initial energy of 3.5 eV and 52 Å for 9.5 eV. The latter shift (and not the former as one would wish) agrees with measurements by means of scanning tunnel microscopy. The penetration of atoms into the bulk of the support takes place in the first 0.2 ns, whereupon the number of inserted atoms proved to be approximately twice as great as the number observed experimentally. The possible role of nonadiabatic transitions in the diffusion of adsorbed atoms on the surface was not discussed in the above studies.[79–82]

MD studies on surface diffusion have not yet received due recognition. Thus, in a review[83] where the results obtained with the aid of scanning tunnel microscopy for the motion of atoms on different surfaces are analysed, no mention whatever is made of molecular dynamics. It was actually claimed that "surprisingly little is known about the mechanisms of the motion of atoms on the surface". Yet one of the main purposes of MD is in fact the study of such mechanisms of dynamic processes.

5. Interaction of clusters with surfaces

Recently much attention has been devoted to the MD modelling of the processes involving the incidence of atomic and molecular clusters on the surfaces of solids.[84–92] Studies have shown that the cluster–support collisions are not described by simple analytical models, since no account is taken in the latter of the collective effects of interatomic interaction. This is the reason why MD modelling is required.

The scheme used in such modelling does not in essence differ from that described above for the incidence of individual atoms (molecules). On the other hand, the choice of the interparticle interaction potentials depends on the energy of the incoming clusters and the energies of the particles in the final state. The entire range of energies investigated is arbitrarily divided into two regions: high energies (> 1 keV atom^{-1}) and low energies (< 1 keV atom^{-1}).

In the first case, problems such as that of the possible appearance in the collision zone of conditions for an appreciable release of neutrons[84,85] or for the excitation of the internal electron shells of the atoms[86] are investigated. Here the relatively short times after the incidence of the cluster are important, during which the highest concentrations of energy are attained and the result is determined by close pair collisions of the atoms. Comparatively simple pair repulsion potentials are therefore selected.

In the case of low energies of the clusters, the formation and structure (epitaxial, amorphous) of the films arising in the interaction of the clusters with the surface,[87,88] the dependence of the appearance of different structures (films, blobs, craters, insertion zones) on the energy and size of the incident clusters,[89] are investigated as are the angle, size, and velocity distributions of the small clusters dispersed from the surface when ions are incident on it.[90] Here it is necessary to trace the energy relaxation process, sometimes up to the thermal level, so that more realistic and complex, multiparticle interaction potentials are needed.

We shall consider in greater detail the processes of this group in relation to the study of Hsieh et al.[89] The incidence of Cu, Ni, and Al clusters with dimensions ranging from 4 to 92 atoms and energies from 92 to 1000 eV atom^{-1} on the surfaces of the same metals in various combinations was investigated. The inserted atom potentials, modified for short distances in order to take into account correctly the collisions of atoms having high energies, were employed.

Depending on the size and energy of the clusters, the elastic and chemical properties of the materials, and the ratio of the atomic masses of the cluster and the support, significantly different results were observed for the interaction. The cluster consisting of 92 copper atoms, incident on the copper surface at low energies, can form a blob, whereas at high energies it penetrates the support, inducing its marked deformation. If the energy of the cluster exceeds 25 eV atom^{-1}, surface defects arise in the support. A cluster consisting of 92 aluminium atoms hardly deforms a nickel support, spreading on the latter epitaxially despite the 15% discrepancy between the Al and Ni lattice parameters. For an energy of 1 keV atom^{-1}, several Al atoms break away from the cluster and are either deflected into a vacuum or are scattered on the surface. Ni clusters with an energy of 326 eV atom^{-1} are almost fully incorporated in the aluminium support and form local amorphous zones.

Fig. 7 presents a diagram illustrating the mechanisms of the interactions of clusters with a surface,[89] showing what results should be expected depending on the kinetic energy of the incoming cluster and the bond energies for an atom in the cluster and in the support.

It is essential to note that, in the MD modelling of certain cluster processes by using the potential approach, it is also necessary to exercise caution (see Section III). Thus it has been found[90] that numerical data agree qualitatively with experimental data and with data derived by means of the analytical theory of the energy distributions of the atoms and dimers dislodged from the surface of the copper crystal when an argon ion is incident on the latter. On the other hand, in order to achieve a quantitative agreement with the theory, it is necessary to choose a copper sublimation energy which is much smaller than the experimental value. The authors[90] explain this discrepancy by the 'loss' of some of the dislodged low-energy atoms due to the characteristics of the methods used in the MD experiment.

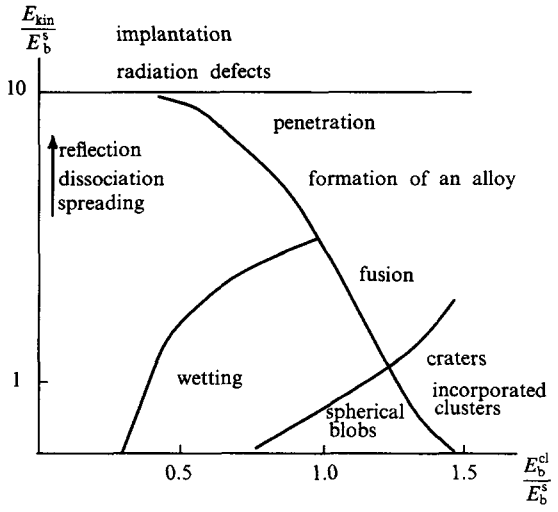


Figure 7. Diagram illustrating the mechanisms of the interaction of clusters with the surface. E_{kin} = kinetic energy of the cluster per atom; E_b^{cl}, E_b^s = the bond energies of the atoms of the cluster and the surface respectively.

However, another interpretation is also possible. If one considers surface + bound atom and surface + free atom states as different electronic states, then the sublimation energy corresponds to the height of the potential barrier between them. As noted in Section III, the interpolated potential surface can model incorrectly the potential barrier between different electronic states. One cannot rule out the possibility that this was in fact the reason for the discrepancy between the qualitative and experimental sublimation energies in the above study.[90]

Insepov et al.[91] investigated the dispersion of the gold surface atoms by argon clusters comprising 87, 141, and 201 atoms. The energy of the cluster was 100 eV atom^{-1}. A method was developed for the removal of the excess pressure arising on impact. The dispersed material of the target consisted of small gold clusters; lateral dispersion was observed.

The limiting case of the spreading of the involatile microblob, present initially on the surface, has been modelled by isothermal MD.[92] Both one-component blobs comprising Lennard-Jones particles and two-component blobs were considered. The second component consisted of a very simple polymer model: a flexible elastic chain consisting of two, four, or eight Lennard-Jones atoms. The total number of atoms in the microblob was $\sim 10^3$. The polymer concentration varied from 0% to 100%. The surface was modelled by a uniform half-space acting on the atoms of the blob via the Mie potential. The initial form of the microblob was specified as a comb periodically extended along its entire length.

The formation of the precursor film was investigated: its width increased initially almost linearly as a function of time and then its growth became diffusional. Its thickness could correspond to the thickness of one or several stepped layers. In the case of polymer solutions, the layers began to mix, which led to their shape approaching hemispherical. The nature of the mixing was investigated for different polymer models and different parameters of the potential. The results agree qualitatively with experimental data.

6. Processes on the surfaces of liquids and polymers

The surface of a liquid differs from that of a solid, apart from lack of order (which incidentally is also characteristic of amorphous solids), also by the fact that it is not as a rule sharp. The density of the surface layer of a liquid gradually decreases from the density of the liquid to the density of the saturated vapour over several intermolecular distances in the liquid.

The scattering of Ne atoms on the surface of glycerol has been modelled[93] for collision energies ranging from 25 to 60 kJ mol^{-1}. The glycerol molecule was described by a nine-centre model, which makes it possible to take into account the torsional flexibility. The hydroxyl hydrogen atoms were included explicitly in the model, i.e. the hydrogen bonds appeared directly. The intramolecular potential energy was expressed approximately by the sum of the Coulombic and Lennard-Jones pair interactions and also by torsional terms. The intermolecular interaction was represented by the sum of Coulombic and Lennard-Jones pair-additive terms. The Ne-glycerol interaction involved only the Lennard-Jones interaction. The glycerol surface at $T = 300$ K was modelled by a cubic cell comprising 343 glycerol molecules with two free surfaces along the z axis. A vaporised glycerol molecule was not observed (the melting point is 291 K).

The sticking, reflection and desorption coefficients of the Ne atoms after several collisions were calculated. The energy losses and the energy and angular distributions were found for the reflected Ne atom. The results agree satisfactorily with experimental data. When an attempt was made to describe the results with the aid of a simple binary collisions model, a decrease in the effective mass with increase in the collision energy was observed. This has been explained by the influence of multiple collisions and by vibrations of the liquid. Data on the energy transfer in the liquid were obtained. The collision energy passes to translational and rotational modes and, to a lesser extent, torsional modes. The energy is then rapidly distributed among the neighbouring glycerol molecules.

Ahlström and Berendsen[94] modelled a L-didecanoyllecithin (an example of an amphiphilic molecule) monolayer on the surface of water. The area of the surface was chosen so that 42 lecithin molecules were accommodated on it. The thickness of the layer of water molecules was 4 nm. The water layer was covered by lecithin from below and from above. The density profiles, the surface tension, and the electrostatic surface potential were found. Local penetrations of water molecules into lecithin were observed. The water-lecithin contact surface is very large and disordered. The results proved to be extremely sensitive to the form of the potential energy for lecithin.

Computer modelling of the dynamics of light gases in a 'rigid' dense polymer matrix exhibits apparent discrepancies with experimental data. Modelling shows that light atoms and molecules (H_2, He) easily attain the diffusional regime, whereas the mobility of heavy atoms and molecules proves to be low. The authors[95] conclude that the 'rigid' matrix is an inadequate representation of the dense system comprising polymer molecules. A qualitative agreement with experimental results can be attained by taking into account the influence of the thermal vibrations of the polymer molecules on diffusion.

VI. Chemical reactions in terms of the adiabatic approximation

1. The use of potential surfaces.

Etching. The chemical interaction of fluorine atoms[45] and molecules[96] with a reconstructed Si(100)-(2 × 1) surface has been modelled. The temperature of the surface of the incident atoms was 300 K. Use was made of the SW type interaction potentials (Si-Si, Si-F, F-F), the parameters of which were chosen in order to achieve agreement with independent experimental data. Sticking, the dissociation of molecules on the surface, the formation of various compounds between fluorine and silicon, etc. were investigated. Hypotheses concerning the etching mechanisms were put forward.

It was observed[45] that, when there is less than one monolayer of F atoms on the surface (surface coverage $\theta < 1$), three outcomes of the incidence of a F atom on the Si surface are possible:

(1) recoil (30%);

(2) chemisorption (the capture of a F atom at the site of rupture of an Si–Si dimer bond or capture by a free bond (60%);

(3) physical sorption (the capture of a F atom by the surface as a whole with retention of the mobility of the F atom along the surface) (10%).

When the coverage of the Si surface by F atoms ranges from $\theta = 1$ to $\theta = 1.25$, the structure of the Si–F surface layer is ordered and stable. There is then no chemisorption, i.e. the physically adsorbed atoms do not penetrate into the bulk of the surface layer and do not form chemical bonds with silicon atoms.

For $\theta > 1.25$, the ordered state of the first adsorbed F layer (illustrated schematically in Fig. 8) becomes unstable. The mutual repulsion of the F atoms distorts the structure. The surplus F atoms can penetrate into the bulk of the surface layer and can break the bonds between the silicon atoms with formation of the complexes SiF, SiF_2, and SiF_3. Subsequently the complex SiF_3 can combine with yet another F atom to form the volatile SiF_4 (etching).

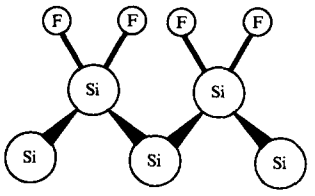
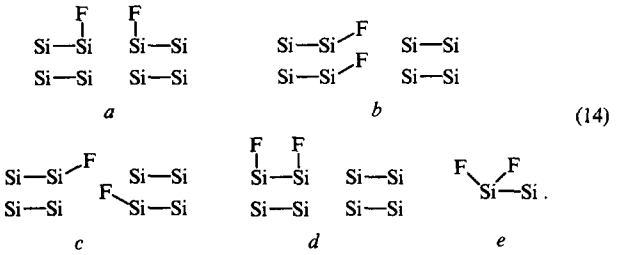


Figure 8. The ordered state of the adsorbed fluorine atoms on silicon.

The overall conclusion of the above study[45] is that, in order to attain the highest rate of etching, the greatest possible disorder of the initial surface is required.

Two main paths in the interaction of an F_2 molecule with the Si surface have been observed[96] — the chemisorption of one of the F atoms and the recoil of the other or, more rarely, the chemisorption of both atoms of the dissociated F_2 molecule. In addition the formation of the Si–F–F complex, where the second F atom is weakly bound to the rest of the complex, has been noted. Rare instances of the reflection of F_2 molecules have also been detected (10^{-3}).

Two chemisorbed F atoms form different combinations of chemical bonds with the Si atoms of the dimers. These bonds can be illustrated schematically as follows:



(14)

Evidently the F atoms can be linked to neighbouring Si atoms belonging to two dimers of different rows (*a*) 'opposite' configuration), two dimers in one row (*b*) 'adjacent' configuration), two dimers in different rows with a displacement by one dimer (*c*) 'diagonal' configuration), one dimer only (*d*) 'the same' configuration). Case (*e*) corresponds to the complex SiF_2.

The numerical probabilities calculated by the MD method can be questioned (see Section III), but the dry etching model agrees qualitatively with experimental data. The study of the role of the removal of heat in the interaction of fluorine molecules with a silicon surface has been initiated.[97]

Surface photochemistry. The dynamics of the surface photochemistry in the system comprising HBr molecules adsorbed on the LiF(001) surface and $\hbar\nu$ quanta has been investigated.[98] The interaction on the surface of the product of the photolysis (H atoms with an energy of 2.6 eV) with H′Br molecules (H and H′ denote simply different hydrogen atoms) has been investigated by the method of classical stochastic Tully trajectories.

$$\mathrm{H'} + \mathrm{HBr} \longrightarrow \begin{cases} \mathrm{H'Br} + \mathrm{H} \\ \mathrm{HH'} + \mathrm{Br} \end{cases} \qquad (15)$$

The interaction energy was specified by the London–Eyring–Polanyi–Sato potential supplemented by the electrostatic and nonelectrostatic potentials of the interaction of the adsorbed atoms with the surface and with one another.

The probabilities of the occurrence of the reactions via paths (15) were investigated, the energy and angular distributions of the H′ atoms were found, and the dependences of these quantities on the surface coverage and temperature were determined. A decrease in temperature increases the probability of the reaction at low coverages and diminishes it at high coverages ($\theta > 0.5$). This effect has been attributed to the formation of a cellular structure of the adsorbent.

Discussion. In the studies considered above and many similar ones, both the results of the dynamic process and the process dynamics itself were investigated. There are no grounds for doubting the reasonableness of this approach to the determination of equilibrium properties — energies, configurations, structures, etc. The process dynamics also has a physical signifiance when one investigates processes occurring on the same potential surface, as specified, for example, in formula (15). As regards processes in which the initial and final stages of the system belong to different electronic states and their wave functions cannot be obtained from one another by any adiabatic alteration of the coordinates of heavy particles, the MMD constitutes for such processes a computational procedure for the determination of the properties of the system in the final equilibrium states. On the other hand, the correspondence of the dynamic process itself to real quantum dynamics requires at least a careful discussion. However, such processes are not even considered in these investigations.

2. Quantum adiabatic calculations

The Car–Parrinello method has been used[100] to investigate the vibrations of hydrogen atoms chemisorbed on the Si(111)–(1 × 1) surface. Fourier analysis of the MD trajectories made it possible to determine the frequencies of the surface phonon mode and to observe an anharmonic relation between the Si–H vibrations and the lower-frequency mode of the surface phonons. The calculated frequencies agree well with the experimental values (except one). The dispersion curves are also close to the experimental ones.

Since the publication of the Car–Parrinello method, investigators made considerable efforts to reduce the expenditure of computer time. One approach involves the improvement of computational schemes (see, for example, Gibson and Carter[101] and Tuckerman and Parrinello[102]). In another approach the number of particles treated quantum-mechanically is reduced and they are surrounded by classical atoms, i.e. a special selection of boundary conditions is made. As an example, we shall discuss a study[103] where the adsorption of the ethyne molecule on the Si(100)–(2 × 1) was modelled.

The basic cell consisted of 360 silicon atoms arranged in ten layers (Fig. 9). The first six layers of atoms moved in accordance with Newton's equations, the seventh, eighth, and ninth layers modelled the removal of heat, and the tenth layer, comprising stationary atoms, bounded the cell from below. Periodic boundary conditions were imposed along the x and y axes. The central group of atoms (quantum cluster), comprising 35 silicon

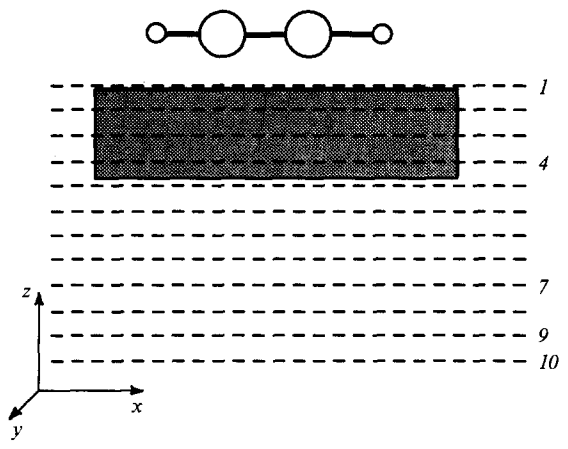


Figure 9. Schematic representation of the basic cell. The quantum cluster is shown shaded: (*1*) – (*10*) numbers of the layers.

atoms in the first four layers (the shaded region in Fig. 9), was examined quantum-mechanically, whilst the remaining atoms interacted with one another in accordance with a potential of the SW type (classical approximation). The problem of the interaction of the "quantum-mechanical" atoms with the "classical" atoms surrounding them was specially solved.

Two configurations of the quantum cluster were considered. The surface layer in a planar projection for the first configuration is illustrated in Fig. 10*a*, while the second layer is show in Fig. 10*b*. The crosses denote the region of incidence and the possible orientations of the C_2H_2 molecule. The first configuration modelled the incidence of C_2H_2 on the dimer or within a row of Si dimers, while the second modelled the incidence between the rows of dimers.

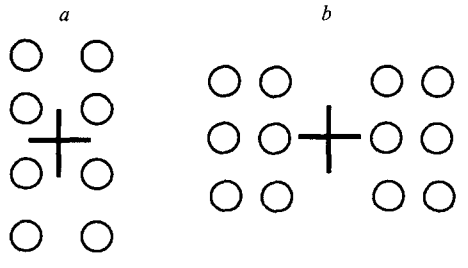


Figure 10. The surface layer of a quantum cluster in plane form. Incidence on a row of dimers (*a*) and between rows (*b*).

The dynamics were considered as follows. With the aid of one of the semiempirical quantum-mechanical methods, the ground electronic state of the system was found: a quantum cluster of Si atoms + C_2H_2 molecule, i.e. a system consisting of 35 Si atoms, two C atoms, and two H atoms. (Additional hydrogen atoms were actually introduced in order to eliminate surface effects — in order to "close" the free valence bonds). The forces found from the quantum-chemical calculations and from the SW potential were then used in Newton's equations, the new positions of all the atoms in the nine layers were found (Fig. 9), and the procedure was repeated. The dynamics of the physical and chemical sorption was investigated in this way, the time characteristics of the interaction were found, and the bond energies and the geometries of the resulting equilibrium configurations were determined.

In the case of a coaxial incidence of the C_2H_2 molecule on the silicon dimer in the geometry presented in Fig. 10*a*, the formation of chemical compounds between C_2H_2 and the silicon surface containing both one σ-type Si – C bond (Fig. 11*a*) and two such

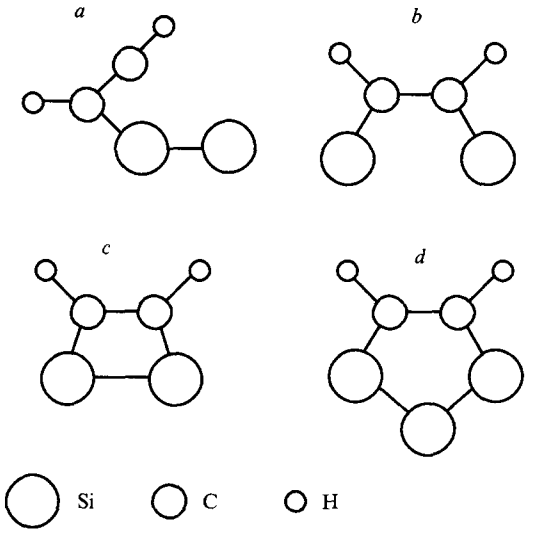


Figure 11. Schemes explaining the formation of chemical compounds between C_2H_2 and the Si surface: (*a*) the formation of one bond with the Si – Si dimer; (*b*) the formation of two bonds with dissociation of the Si – Si bond of the dimer; (*c*) the formation of two bonds without the dissociation of the Si – Si bond of the dimer; (*d*) the formation of a bridged compound.

bonds (Fig. 11*b*) was observed. In the case of the configuration shown in Fig. 11*b*, the Si – Si bond in the dimer was broken. This bond could then be restored without the dissociation of a Si – C bond, but this configuration (Fig. 11*c*) proved to be unstable. After several transitions from the configuration 11*b* to 11*c* and conversely at 100 – 400 fs intervals, the collision configuration 11*b* was established.

The result of the incidence of C_2H_2 depended strongly on the site of incidence. On incidence between neighbouring dimers of the same row, when the axes of the dimer and C_2H_2 are mutually perpendicular (Fig. 10*a*), the bridged configuration 11*d* may be formed. On incidence of C_2H_2 between neighbouring rows of dimers (Fig. 10*b*), bridging configurations were not observed. Only physical sorption was noted and the axis of the C_2H_2 molecule was arranged almost parallel to the surface of silicon. In the case of the migration of C_2H_2 onto the row of dimers, the configurations already considered in Figs. (11*a*) and (11*b*) were formed. The dependence of the outcome of the incidence on the orientation of the molecular axis of C_2H_2 relative to the axes of the dimers was no less marked. For a nonparallel arrangement, the ethyne molecules were reflected.

The criticisms expressed in the previous subsection retain their force in this case too. Indeed, the authors themselves[103] present a plot analogous to that shown in Fig. 1. The physical and chemical sorptions are described by different potential curves (curves *2* and *1*) corresponding to different electronic states. In fact, the calculations[103] are performed for curve *3*, joining both local minima. Thus the dynamics of the transition from physical to chemical sorption within the framework of the above approach[103] is described with the aid of Newton's equations for a single potential surface. However, in actual fact this transition is electronic and should be described by the non-stationary Schrödinger equation. We may note that it is seen from Fig. (11) that a whole series of chemisorption states are possible, i.e. there should be several type *2* curves in Fig. 1 in this case.

However, these questions were not even mentioned in the above study.[103] Thus the time characteristics obtained[103] may not correspond to reality. On the other hand, the equilibrium characteristics of the final state do not give rise to such doubts — the formulation of the problem of their determination is correct and the error may be due only to the approximate nature of the computational procedure or $\Phi(R)$.

VII. Nonadiabatic quantum molecular modelling

Sections II – VI led to a paradoxical conclusion: both the classical and quantum MMD may prove to be inadequate precisely in those applications for which they have been in fact generally speaking designed — for the calculation of the dynamics of the transitions between different states. Such calculations require the solution of the nonstationary Schrödinger equation. The numerical methods for the integration of this equation have been the object of intense investigation (see, for example, Refs 5 and 104 – 110 as well as the references contained therein). By themselves, these methods have no bearing on the MMD, which is based on the calculation of trajectories, although they can be combined with it in order to solve quantum problems, as will be shown below.

Molecular dynamics with electronic transitions. A series of studies associated with Tully's name have been devoted to this question.[5,104–106] We shall explain the idea of the method by means of a schematic example (Fig. 12). Suppose that a particle is reflected during adiabatic motion along trajectory *1*. If the particle causes the excitation of the surface of a solid, it loses part of the energy, a nonadiabatic electronic transition takes place, and the particle trajectory (curves *2*) changes, in particular sticking may occur.

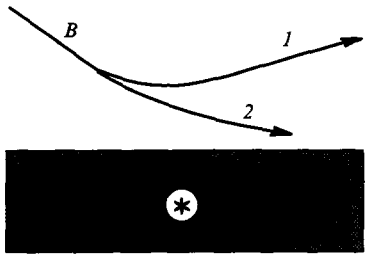


Figure 12. Scheme explaining the splitting of the trajectory in electronic transitions. The star denotes the excitation of the surface.

It is clear from the foregoing that the branching of the trajectories is a distinctive feature of MD with electronic transitions, which has already been discussed in Section III (the potential picture in Fig. 1*b* corresponds to Fig. 12). No jumps in space occur under these conditions, the concept of the trajectory is retained, and the latter remains smooth, but at point *B* the trajectory no longer satisfies Newton's equation. Since the electronic transition has a probability, it is necessary to generate a family of trajectories with the same initial conditions. The frequency of the appearance of points *B* and their spatial distribution are then modelled.

In the general case, the problem involves the nonstationary Schrödinger equation for a quantum particle or a subsystem of particles, the transitions between different adiabatic potential surfaces, and Newton's equations for heavy particles. The Schrödinger equation can be approximately reduced to ordinary differential equations for the expansion coefficients of the wave function in terms of stationary states, the coefficients being time-dependent in the given instances. Newton's equation includes the response of heavy particles to electronic transitions in the quantum subsystem.

In view of the complexity of this problem, solutions have so far been found only for certain special cases. Thus one-dimensional two-level methodological examples have been considered.[5] In other studies,[104,105] a series of results have been obtained for the solvated electron. The study of Webster et al.[106] was devoted to further development of the method and to a methodological two-level example.

In order to illustrate the role of nonadiabatic effects, Dodson[4] carried out the MD modelling of the incidence of silicon atoms onto a silicon support for a single energy (12.5 eV) and two interaction potentials of the incoming atom with the surface atoms: a type SW potential described the adiabatic case and the Ziegler – Biersack – Littmark potential described the case of the complete rupture of Si – Si bonds. The results proved to be very different: thus the depth of penetration of the Si atoms into the surface layer was 2.8 Å in the first case and 10.5 Å in the second.

Tunnelling. It has been noted[5] that this process can be investigated separately from electronic transitions, since the probability of the latter decreases, according to Massey's criterion, with increase in the velocity and is independent of the mass of the particles, whereas the role of tunnelling increases with decrease in velocity and in mass. The object of study was the dissociation of hydrogen molecules on a surface.

The dissociation of H_2 on copper has been considered.[107] In view of inadequate computer capacity, the quantum calculations were restricted to the case of a two-dimensional potential surface. Although the influence of quantum effects on the sticking coefficient was in fact noted, a satisfactory agreement with experiment was attained only on passing to a six-dimensional description of the potential surface within the framework of quasi-classical molecular dynamics.

The grid method was used for the numerical integration of the time dependent Schrödinger equation.[107] In this case, the computation time is proportional to N_g^D, where N_g is the number of points in the grid and D is the dimensionality (the number of degrees of freedom). The nonstationary problem has been solved[108] with the aid of the multiconfiguration Hartree approximation with a natural choice of one-particle states. The computation time proved to be proportional to $N_g^{D/2}$. However, only a two-dimensional model of the dissociation of H_2 on the surface of a generalised transition metal was considered as an example.

An approximate approach, which made it possible to model the dissociation of the hydrogen molecule when it is incident on the Cu(110) surface, has been proposed.[109] The interaction surface of the $H_2 - Cu(110)$ system was six-dimensional. It was found by using the inserted atom method and for H_2 it was brought into correspondence with the LEPS surface. The probability of sticking (α) and the free energy activation barrier (ΔF) were found in terms of the approximation of the quantum theory of the transition state (TTS):

$$\alpha = \exp(-\beta \Delta F) , \tag{16}$$

$$\Delta F = -\int_s f \mathrm{d}s , \tag{17}$$

where s is the trajectory of the hydrogen molecule and f the average force acting on this molecule taking into account the quantum dispersion. The principal TTS approximations are as follows: (1) the inequality $\alpha \ll 1$ must hold for Eqn (17) to be valid; (2) in the phase space of the $H_2 - Cu(110)$ interaction there must be a narrow place which would make it possible to determine clearly the hypersurface separating the region of the initial state (the H_2 molecule) from the region of the reaction product (the H + H atoms); (3) (the main approximation) when the trajectory s of the H_2 molecule intersects the separating hypersurface, determined on the basis of the preceding assumption, the dissociation of H_2 is assumed to have occurred. Thus the integration in Eqn (17) is carried out from the distance where the $H_2 - Cu$ interaction can be neglected up to the intersection by the separating hypersurface.

For the calculation of ΔF by Eqn (17), the following approximate procedure has been proposed.[109] The minimum energy path which smoothly and continuously transfers the system from the initial to the final state is found. This is carried

out by a novel method, developed by Mills and Jonsson,[109] whereby the trajectory s is obtained. Five-dimensional hypersurfaces perpendicular to s are determined in succession along this trajectory. For each surface, the average force f acting on the H_2 molecule located on this hypersurface is found. The calculations are repeated until the hypersurface with $f = 0$ is reached. After this, the integral (17) and then α are found.

All the quantum effects are contained in the force f. In order to determine the latter, the formal treatment involving integrals along the trajectories, already mentioned earlier in connection with molecular modelling, is resorted to.[12,111] The representation of the partition function, proposed by Feynman, in the form of a Wiener integral along the 'trajectories'¶ is employed. Its finite-dimensional approximate representation has the same form as the classical partition function for a cyclic system of linked identical harmonic oscillators with an elastic constant determined by the mass of the particle, temperature, the constant $\hbar$, and the number of subdivisions of the cyclic 'trajectory'.¶ The 'trajectory' characterises the quantum dispersion of the H atom and is specific to each H atom.

Thus, in order to find the quantum dispersion and the average value of f, one may carry out the classical MD modelling of the motion of a cyclic chain of linked oscillators for each atom. The centre of gravity of both chains is then retained by force on the chosen hypersurface. The classical limit of the modelling corresponds to the contraction of the chains into a point on the trajectory s. In addition to hydrogen atoms, such modelling has been carried out for the eight copper atoms closest to the H_2 molecule. The chains consisted of 50 units.

The results of the calculations showed that the quantum effects begin to exert an influence at a temperature below 600 K, where the delocalisation of the hydrogen atoms is manifested, leading to a decrease in the effective activation energy $E_a = \partial(\beta\Delta F)/\partial\beta$ from 0.70 to 0.45 eV. However, the absolute value of $\beta\Delta F$ proved to be somewhat too high. This yielded an unduly low sticking coefficient ($\alpha = 1 \times 10^{-7}$) compared with the measured value ($\alpha = 4 \times 10^{-6}$) at 600 K. The authors[109] attributed the difference to the inaccurate choice of the H_2–Cu model potential surface.

Calculations with frozen vibrational and rotational degrees of freedom showed that the excitation of these degrees of freedom does not play a notable role. The principal quantum effect is delocalisation; the authors[109] attribute the 30% decrease in the energy of activation in the quantum region to tunnelling by the hydrogen atoms.

New numerical approaches to the solution of the nonstationary Schrödinger equation have been considered by Pollard and Friessner.[110]

Trajectory approaches. It is seen from the preceding sections that new molecular modelling methods are continuously being sought for nonstationary quantum problems. Frequently these methods are supplemented by the MMD.

At the same time attempts have been made to devise methods for the numerical solution of the time quantum problem, which are related to the classical MD and are based on the trajectory interpretation of quantum mechanics. The approach, proposed by Podlipchuk[112,113] in studies where a stochastic ordinary differential equation in a complex space was obtained instead of the nonstationary Schrödinger equation for the description of the quantum assembly, is promising. Here it is in fact numerically much simpler to carry out the nonstationary process than to seek stationary states.

A new variant of quantum molecular modelling of time quantum processes, in which the Wigner formulation of quantum mechanics is employed, has been proposed.[114] A combination of the classical MMD and the Monte Carlo method, analogous to the Monte Carlo method developed in statistical dynamics, was used for the solution of the Wigner–Liouville equation.[12] Systematic calculations were performed for the motion of the electron in a one-, two-, and three-dimensional potential well with and without a barrier. The time dependences of the quantum-mechanical average values of the coordinate and momentum, their dispersions, and energy were calculated. Test calculations for a low-energy particle on the bottom of the well yielded results in good agreement with the analytical solution in terms of the harmonic approximation. The rate of tunnelling through the barrier was found by calculating the trace of the operator of the autocorrelation function of the momentum.

VIII. Transition from dynamic to probability modelling

The dynamic methods examined in the previous section proved to be a powerful and flexible instrument for the investigation of a wide variety of elementary processes on the surface. However, a number of difficulties arise in the application of these methods to chemical modification problems. The most evident are the limitations as regards the speed and memory of the computers.

Material limitations of the dynamic methods. The technologically important scales of the surface modification processes are $\tau \sim 1$ μs in time and $l \sim 1-10$ μm in length. Modern computers permit classical MD modelling for times $\tau < 1$ ns and in terms of the length scale $l < 100$ Å. For quantum dynamic modelling, these quantities are even smaller. The limiting possibilities of the existing computers are then employed. Clearly the possibilities of modelling lag by orders of magnitude behind the requirements.

We may note that the current attempts to model, for example, the deposition process employ unrealistically short time intervals between the steps involving the incidence of particles on the surface.[4] On the one hand, this makes the rate of growth of the surface be of the order of magnitude of the speed of sound. On the other hand, the shortening of the time interval between elementary steps distorts the state of the surface which participates in the next elementary step.

Optimists may assume that these are temporary difficulties at the present stage of the development of the computer techniques. Whatever is the truth, there nevertheless are serious limitations which make the task of expanding the scale of the purely dynamic modelling of the chemical modification of surfaces pointless.

Fundamental limitations of the dynamic methods. Chemical reactions with electronic transitions play an important if not the principal role in the chemical modification of the surface. As shown in the previous sections, such processes cannot be modelled with the aid of the classical and adiabatic quantum MD.

Quantum-mechanical approaches based on the solution of the nonstationary Schrödinger equation have been developing for the study of such problems (electronic transitions, tunnelling, etc. — see Sections VI and VII). These methods impose even more severe requirements on the computer resources, particularly in the study of surfaces.† However, this is not the most important factor. The main feature is the appearance of a new qualitative element in such modelling. In the course of the computation, it becomes necessary in fact to make a choice between mutually exclusive possibilities ("splitting" of the trajectory). In the case of a surface, these are, for example, variants of the behaviour of the

¶ The 'trajectory' lies on the five-dimensional surface already discussed above and should not be confused with the trajectory s. For this reason, we place it in quotation marks.

† Apart from the microscopic quantum interactions involving several particles, 'macroscopic' interactions, not localised in space, are significant in this case. The reconstruction of a large section of the surface induced by the incidence and adsorption of a single atom may serve as an example.

particle (adsorbed atom) after its physical adsorption. The adsorbed atom can change its location whilst remaining a physically adsorbed particle, chemical bonds may be formed between the adsorbed atom and the surface atoms, which is accompanied by electronic transitions, and, finally, there is a possibility of quantum diffusion, thermal desorption, etc.

Thus in molecular modelling which uses the nonstationary Schrödinger equation, the extent to which the process is determined is inevitably weakened because at the branching points the choice of the variant is probabilistic in character. This is not associated with the numerical schemes for the solution but is due to the physical significance of the quantum mechanics itself. Indeed, the determination of the state of a quantum system makes it necessary to make a measurement (reduction of the wave packet), i.e. to pass from the probability amplitude (wave function) to the probability density (square of the modulus of the wave function). In a series of measurements, the results will be distributed in accordance with this probability. Such a series of 'measurements' is in fact performed in quantum modelling.

We may note that the classical MMD is also not in fact purely dynamic.[7-9] As a consequence of the instability of the equations of motion for a system of many particles and the errors in the numerical integration, which play the role of perturbations, the MMD trajectory deviates exponentially from the Newtonian trajectory for the same initial conditions, remaining close to the latter only for relatively short times. For long computational times, the MD trajectory moves under these conditions from one set of sections of the Newtonian trajectory to others, which are 'dynamically remote'. These transitions are probabilistic in character because many-particle systems are of the mixing type.

In nature, the phase trajectories of molecular systems, which can be regarded as classical, are also continually perturbed (for example, because any such system is open). For this reason, the motion of such systems is also stochastic in character.[10,11]

It is clear from the foregoing that the need to resort to probability methods in molecular modelling is predetermined by the very physics of the problem. On the other hand, the attempts to remain within the framework of 'pure' dynamics particularly in calculations for large time scales, are not simply unproductive but are in essence pointless.

Probability methods. Since probability modelling is inevitable in the key stages of the solution of the problem, it is useful to exclude altogether from consideration the long sections of the dynamic phase trajectories without an information content. This is possible when the time intervals between successive incidences of the particles on the surface are much longer than the time required for the transition of the system to a new stationary state (the overall time of the chemical reactions, reconstruction, dissipation of excess kinetic energy, etc.). The dynamic methods are retained for the calculation of the probabilities of elementary processes (sticking, chemical reactions, reconstruction shifts, etc.). Knowing the possible states of the system as well as the probabilities of the transitions between them, the kinetic calculations for these transitions can be performed by the Monte Carlo method.

Such an approach makes it possible, in principle, to shorten the computation time by several orders of magnitude, firstly by accelerating the 'selection' of the elementary steps and, secondly, as a result of the fact that the required probabilities should be ideally determined 'once and for all'. However, the multiplicity of the individual surface geometries (steps, groups of adsorbed atoms, vacancies, etc.) is extremely large. It is virtually impossible to guess all the states of the system during its evolution and to calculate beforehand the probabilities of the transitions for these states. It is therefore necessary to have in addition a simple and at the same time an acceptably accurate method for the determination of the electronic structures of the current states of the system and hence the transition probabilities. The method must be applicable in the probability modelling process itself. The principles governing the development of this method on the basis of quantum-chemical ideas are described in the preceding sections.

The loss of information about the dynamics of certain transitions is insignificant for the description of the evolution of the chemical modification of the surface, provided that the rate of modification is determined by the rate of arrival of the reagent on the surface. The knowledge of the times of individual transitions is important in order to be able to discover in which cases this is really so.

Thus it is possible to devise an algorithmic scheme modelling the real shape formation for fairly large crystal specimens. This algorithm must contain the following elements: (1) fragments of the dynamic description; (2) the determination of the stationary states and the probabilities of the transitions between them; (3) the modelling of the probability processes for these transitions (the Monte Carlo method). This modelling procedure constitutes a combination of the MD, quantum-chemical, and Monte Carlo methods.

The dynamic and probability methods were previously compared in attempts to discover which of them is more effective.[4] In fact, they are complementary and their joint employment intensifies the strong aspects and eliminates certain weak aspects of each method.

IX. The simplest probability models. Cellular automata

1. Discrete modelling. Morphology of the surface

The crystal is specified within the framework of the lattice model, a proportion of the crystal lattice sites located on the boundaries of the crystal being assumed vacant. In the simplest models, the crystal lattices are considered in an extremely simplified form (frequently with a smaller dimensionality).

The set of the possible outcomes of the elementary process is determined. The location of the elementary step on the surface is selected at random. The process reaches its conclusion at this point, with the aid of a priori specified probabilities, the crystal is then prepared for the next step, etc. Whatever its form, this procedure is applied in all the simplest models of the chemical modification of the crystal surface considered in this section. Sometimes a model procedure of this type is referred to as cellular (lattice) automata.[115,116]

This aspect may be called morphological because the study of the modification is limited to the 'geometrical' modelling of the morphology and only phenomenological ideas concerning the process on the surface are used. However, the principal concepts and ideas — the language in which one may speak of the form of the surface of the crystal — were formulated in this connection.

Among the studies concerned with this aspect, we may name the simplest models of random deposition.[117-119] The surface is characterised by concepts such as 'coarseness' (roughness, thickness). It has been found that the dispersion of the height of the surface formed (a measure of its roughness) is proportional to the square root of the height of the deposited layer.

The ballistic deposition models,[120-122] describing the appearance of projections, holes, and shadows, may be mentioned as more complex ones. A power dependence of the thickness of the surface not only on the height of the deposited layer but also on the linear dimensions of the support appears. The statistical modelling of various formations with dimensionalities equal to unity or 2 — strings, terraces, etc. — becomes possible.[121-123]

The development of discrete models is virtually completed by the studies described in Refs 124-126 — the transition to the consideration of specific chemical properties begins with the appearance of new information about the surface. The study[127] in which the kinetics of the growth were modelled on the basis of the local properties of the surface being modified is typical. Such properties, in particular the differences between the energies of the surface and bulk-phase atoms, have been calculated[128] in the

form of the stress tensor. Further development should follow the path involving the modelling of chemical bonds.

The simplest models make it possible to represent the way in which the form of the crystal changes and to specify which characteristics describe it sufficiently completely and at the same time are susceptible to investigation. However, the possibilities of such modelling are extremely limited. Firstly, no account is taken of the dependence of the probabilities of the elementary processes at any point on its local environment. Secondly, the set of elementary processes specified a priori does not exhaust the true diversity of the real processes.

2. Continuous modelling

In this approach, the form of the surface is considered as a continuous function $H(r, t)$ of the spatial coordinates and time. The processes involved in the establishment of equilibrium have proved extremely important. There are two limiting cases. In the thermodynamic limit, the surface modification process is infinitely slow so that there is sufficient time for the attainment of thermodynamic equilibrium after each modification step. In this limit, $H(r, t)$ represents either a flat surface or a system of projections and hollows along thermodynamically stable crystallographic faces. The other limit is kinetic. In this case, the modifying particles land so frequently that there is insufficient time for the occurrence of the material transfer processes along the surface between successive collisions.

The real process is always of an intermediate type, i.e. the rate of landing of the modifying particles is finite and the tendency of the form of the surface to attain the thermodynamic equilibrium form is distorted by kinetic processes.

The equation of the surface $H(r, t)$ assumes the following simplest form:

$$\frac{\partial H(r,t)}{\partial t} = \eta(r,t) + \hat{A}\{H(r,t)\}, \tag{18}$$

where $\eta(r, t)$ is a random source describing the variation of the roughness of the surface during the deposition process or during etching as a result of the discreteness of the elementary steps. The operator $\hat{A}$ describes the influence of the smoothing or other shape-forming factors of the type of three-dimensional or surface diffusion. The competition between the processes involving the formation of the locally rough surface and the formation of a gentler relief is the main cause of the diversity of the forms of surfaces.[129-130]

On the most general hypotheses concerning the type of the second term of Eqn (18), one may investigate the degree of roughness of the surface being modified by determining $w_L^2(t) = (H - \bar{H})^2$. This quantity exhibits different scaling behaviour depending on the lengths L with respect to which averaging is carried out.[130-132] For small values of L, this quantity is almost independent of time and is determined solely by the value of L, while for large L it ceases to depend on the averaging length and depends solely on the observation time:

$$w_L(t) \sim \begin{cases} L^{\alpha}, & L \ll L_c \\ t^{\beta}, & L \gg L_c \end{cases} \tag{19}$$

The boundary L_c between the regimes depends on time: $L_c \sim t^{\beta/\alpha}$.[130] In the thermodynamic and kinetic limits, the exponent α should become zero (the quantity w_L in the limiting cases should be independent of the averaging length). On attainment of thermodynamic equilibrium, the exponent β should also become zero (the causes giving rise to a time dependence are absent in this case). In the kinetic limit, the function $H(t)$ should obey the standard Poisson distribution and hence $\beta = \frac{1}{2}$.

One may expect that, for specific models of the surface modification, the exponent α varies nonmonotonically on transition from the thermodynamic to the kinetic case and reaches a nonnegative maximum at some point. On the other hand, the quantity β apparently varies monotonically — in the kinetic limit the time variation is a maximum, so that the real value of β is in the range $0 < \beta < \frac{1}{2}$.

The constants α and β may be determined for different continuous models with a different specific form of the operator $\hat{A}$. They can be obtained also in computer modelling for different discrete models and in experiments on the deposition and etching of crystal surfaces. The scaling exponents yield information about the extent to which the real modification regimes are close to the thermodynamic or kinetic limit. They make it possible to compare the continuous and discrete models of the modification of the surface and also to discover how well particular models describe the real experiments on deposition and etching.

X. Quantum description of the chemical bond on the surface

Elementary ideas. We may recall the simplest chemical system — two hydrogen-like atoms. In terms of the basis set of atomic wave functions, the diagonal elements of the Hamiltonian coincide with the energies of the electronic states in the individual atoms E_1 and E_2, while the nondiagonal elements represent the amplitude of the probability of the transition of the electron from one atom to another (v). The stationary states of a two-atom system are found to be the bonding and antibonding states with the energies

$$E_{a,b} = \varepsilon \pm (\delta^2 + v^2)^{1/2}, \qquad \varepsilon = \frac{E_1 + E_2}{2}, \qquad \delta = \frac{E_1 - E_2}{2}. \tag{20}$$

For the ground states of identical atoms, $E_1 = E_2$ and $E_{a,b} = \varepsilon \pm v$.

When the chemical interaction of a solid with an atom (molecule) is considered, the state of the atom (molecule) remains as one of the electronic states in Eqn (20), while the set of the electronic states of the solid is chosen as the other. The highest occupied electronic states (the states near the Fermi level) play the main role. Eqn (20) reflects the simplified situation where each chemical reactant has one electronic state ready for coupling. In the general case, there are several (valence) states of this kind and Eqn (20) is accordingly also generalised‡.

The atoms which can modify the surface come into contact only with the surface of the crystal, so that the surface electronic states and not the bulk-phase states should be considered as the electronic states in Eqn (20).

The surface of the crystal is reconstructed, i.e. acquires a lower symmetry compared with the case when the atoms on the surface remain at lattice sites. The spontaneous decrease in the symmetry of the crystal surface is a transition of the Jahn–Teller type, in which the coordinates of the surface atoms and the positions of the surface electronic states change. The energies of the occupied and unoccupied surface states as a rule move apart under these conditions.

Examples involving the consideration of chemical bonds. Tomasek et al.[128] deduced the surface states of adsorbed atoms in a very simple way — from the number of ruptured bonds, i.e. without taking into account reconstruction. They suggest that the differences between the interactions of the surface atoms and the atoms in the bulk phase be described phenomenologically with the aid of the stresses tensor. Chadi[133] surveyed the electronic and atomic structures of semiconductor surfaces with low indices — [100], [111], and [110]. The conclusion that the recon-struction of the covalent surfaces is induced mainly by the tendency towards an increase in the bond orders of the surface atoms agrees well with the possibility of describing the

‡ Henceforth, in referring to Eqn (20) this generalised form will be understood.

differences between the surface and bulk phase with the aid of the stress tensor.[128]

Significantly more detailed methods for the description of chemisorption on semiconductor surfaces have also been adopted.[134,135] The molecular orbital method made it possible to calculate the positions of the oxygen atom on the surface of silicon. A quantitative agreement has been achieved between the calculated and experimental vibration frequencies of the oxygen atoms.[134] Zheng and Cao[135] described three stages in the oxidation of silicon: the chemisorption of oxygen molecules, the dissociation of molecular oxygen, and the diffusion of atomic oxygen from the bridging adsorption layer into the bulk of the crystal with formation of an SiO_2 film. However, progress in the understanding of the process has been achieved at the expense of the loss of flexibility and universality of the description. The three-step representation of the chemical reaction hinders the inclusion of this stage of the computation in the algorithm for the modelling of the chemical modification of the cellular automaton type. Indeed, each of the stages of the process requires the processing of a large amount of information and depends significantly on the composition and state of the vicinity of the section being modified.

The energies of the surface states have been calculated[136] for the reconstructed Si(111)-(2 × 1) surface. The dependences of the energies on the magnitude of the reconstruction shifts were obtained. The study of Yamaduchi and Fujima[137] may serve as an example of the calculation of the surface states localised on a step. Their structure is related to the configuration of the atoms on the edge of the step, which consists of a zig-zag chain of dimers.

This approach proved productive in the study of the interaction of ion beams with the surface of a solid,[139-141] where it was assumed that the structure of the electronic states corresponds to the bulk-phase state. The scattering singularities are manifested in cases where the energies of the electronic states of the incoming ion and the crystal are identical. Electron exchange is of the resonance type. Even if chemical reactions do not occur under these conditions, the scattering singularities constitute high-energy echoes of such reactions.

We may note that the scheme of the bulk-phase electronic states of the crystals employed in the studies of Balidchik and coworkers[139-141] is appropriate only when interactions with high-energy particles (hundreds of eV) are considered. In this case, the interaction energy is so high that the details of the electronic structure of the crystal are unimportant — the position of the Fermi level is the most significant feature. For lower energies, the singularities will arise when the levels of the atomic particle coincide with the unoccupied and occupied surface states closest to the Fermi level. When a sufficiently selective diagnostic procedure is available which permitts the resolution of these singularities, their analysis might prove a promising instrument for the study of the electronic states of a reconstructed surface.

The approach to the description of the chemical properties of solids based on the consideration of surface states, reconstruction, etc. has been used in qualitative studies.[138] Unanimity has been achieved in the understanding of many chemical processes on the surfaces of solids.

The studies under discussion§ have led to progress in the description of individual chemical bonds in the bulk phase and on the surface of a solid, but they cannot serve as a basis for universal modelling. For such modelling, it is necessary to find a standard approach to the calculation of the energies of the surface states and the matrix elements in Eqn (20).[142,143]

§We may also indicate the following reviews: G M Zhidomirov, A A Bagatur'yants, I A Abronin. *Prikladnaya Kvantovya Khimiya* (Applied Quantum Chemistry). Khimiya, Moscow, 1979; N P Gambaryan, I V Stankevich. *Usp. Khim.* **58** 1945 (1989) [Russ. Chem. Rev. 1103]; I D Mikheikin, I A Abronin, I K Vorontsova. In *Materialy VI Mezhdunarodnogo Shkoly-Simpoziuma po Khimicheskoi Fizike* (Proceedings of the VIth International School-Symposium on Chemical Physics). MATI, Moscow, 1994, p. 174.

XI. The method based on the generalised periodic system of the elements

1. Massive crystals

A method was proposed by Harrison[14] in a general form for definite groups of elements in the Periodic System. For this reason, the method (or more precisely the set of parameters used in it) is referred to as the generalised Periodic System of the elements (GPSE). For elements forming covalent tetrahedral crystals, such parameters are the lattice constant d, the energies ε_s and ε_p of the s and p electrons in the ground configuration of the atom, and the Fermi momentum k_F. The radius r_c of the non-coulombic component of the interaction is also used for the construction of the pseudo-potential describing the interaction of the valence electrons with the core electrons.

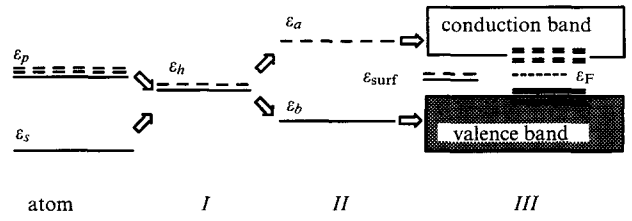


Figure 13. Stages in the construction of the electronic states of a silicon crystal with the aid of the GPSE. Continuous lines — occupied states; dashed lines — unoccupied states. The surface states ε_{surf} are indicated in order to explain Fig. 14.

Fig. 13 explains the essential features of the method. To make the treatment specific, the values of the parameters of the electronic states correspond to silicon. In the first stage, the s and p valence states are hybridised, i.e. a transition to new orthonormalised functions is carried out. They are not eigenfunctions of the Hamiltonian but they do have a symmetry convenient for the description of diamond-like crystals. These states have the same average energy

$$\varepsilon_h = \frac{\varepsilon_s + 3\varepsilon_p}{4}.$$

In the second approximation, account is taken of the overlap of the sp^3-hybridised orbitals in the direction of nearest neighbours only (these are in fact the ones participating in the formation of the chemical bond). The GPSE method involves convenient universal formulae for the overlap integrals. For example, the following expression is used for the overlap integral V_c^h (the energy of the covalent bond involving hybridised orbitals):[14]

$$V_c^h = \frac{-V_{ss\sigma} + 2\sqrt{3}V_{sp\sigma} + 3V_{pp\sigma}}{4},$$

where the subscripts $ij\alpha$ define the atomic (Roman letters) and molecular (Greek letters) quantum numbers. The dependence of the overlap integrals on the distance d is given by the estimate

$$V_{ij\alpha} \approx \eta_{ij\alpha}\frac{\hbar^2}{md^2}, \qquad (21)$$

where m is the mass of the particle. The coefficients $\eta_{ij\alpha}$, where $i, j = s, p, d$ and $\alpha = \sigma, \pi$, have been published.[14] We obtain for the energy of the bonding and antibonding orbitals

$$\varepsilon_{a,b} = \varepsilon^h \pm V_c^h. \qquad (22)$$

For covalent crystals formed by different atoms, for example GaAs or ZnS, a second interatomic matrix element V_i^h (the energy of the ionic bond involving hybridised orbitals) is introduced. It is defined as half the difference between the energies of the hybridised states of different atoms:

$$V_i^h = \frac{\varepsilon_h^A - \varepsilon_h^B}{2}.$$

The energies of the bonding and antibonding states are given by the expression

$$\varepsilon_{a,b} = \frac{\varepsilon_h^A - \varepsilon_h^B}{2} \pm \alpha(d, \varepsilon_s, \varepsilon_p) \ , \qquad (23)$$

where

$$\alpha(d, \varepsilon_s, \varepsilon_p) = [(V_c^h)^2 + (V_i^h)^2]^{1/2}.$$

In the third approximation (Fig. 13), account is taken of the overlap of the orbitals obtained in the direction of the translational vectors.[14] This makes it possible to find the splitting of these levels into valence and conduction bands, to determine the structure of the subbands, and to obtain the dependence of the energies on the quasimomenta k.

The fourth approximation is not fully unambiguous. In the most successful version, the main correction is the matrix element describing the interaction of the valence electrons with the core electrons. For simple metals, such a correction is given by a pseudo-potential, which is regarded as a perturbation. In the case of covalent crystals, the interaction of the valence electrons with the core electrons cannot be regarded as small. Here the wave functions are determined by the maximum Fourier component of such a pseudo-potential with the wave vector along the [111] direction. The additional dependence on k_F and r_c appears only in the fourth approximation.

Somewhat different sets of parameters and other procedures for the construction of the electronic states and for the description of chemical properties have been proposed for other groups of elements — the halogens, simple metals, and metals with an unfilled d or f shell.[14] Thus the GPSE makes it possible to isolate the common features in the description of different groups of substances and to formulate for each of them a procedure analogous to that described above for covalent crystals. Many computational procedures for different groups of elements proved to be similar — LCAO for the construction of valence bands, the approximation of almost free electrons for conduction bands, and the description of the interaction of valence electrons with core electrons with the aid of a pseudo-potential.

2. The surface

a. Surface electronic states

Fig. 14 illustrates the region corresponding to the forbidden band gap *III* in Fig. 13. The surface energy levels are formed in this region. The initial idea concerning the surface state may be the concept of a broken bond arising when some of the atoms are removed from the crystal; the wave functions adopted are those of the sp^3-hybridised state. Neglecting the amplitude of the translational transitions, the energy of such a state may be regarded as identical with ε_h (Fig. 14*a*). Further consideration (allowance for the amplitudes leading to the appearance of bands at the level of the third or fourth approximation) leads to different results depending on the geometry of the interface.

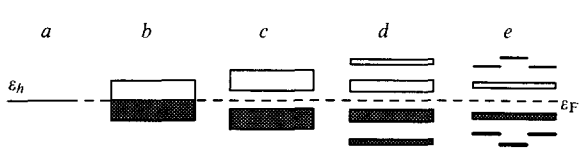


Figure 14. The energy diagrams for surface states: (*a*) crystals with ruptured bonds; (*b*) flat smooth surface; (*c*) reconstructed surface; (*d*) reconstructed surface with regular structures; (*e*) surface with an arbitrary geometry. The occupied bands are shown shaded.

Ideally flat surface. The positions of the atoms in the surface layers coincide with the positions of the crystal lattice sites of the bulk phase crystal and the Miller indices for the surface do not exceed unity. The amplitudes of the transition in the direction of two minimal translational surface vectors can be determined with the aid of the standard GPSE procedure.[14] The solution of the problem of the eigenvalues leads to the appearance of a half-filled band of surface states (14*b*). The energy of these states $\mathscr{E}_0(\mathscr{K})$ depends on the two-dimensional quasi-momentum $\mathscr{K}$, which ranges over the values in the Brillouin surface band determined by the symmetry of the interface.

Reconstruction. Linear structures. The set of reconstruction and relaxation shifts is described by the vector $\vec{\Delta}$. In the simplest case, where the reconstructed surface has two-dimensional translational symmetry, the dimensionality of $\vec{\Delta}$ is $3 \times m$, where n is the number of atoms in the surface unit cell for the nonreconstructed surface and m is the number of nonreconstructed cells in the reconstructed surface (we restrict the treatment to the approximation where the displacement of surface atoms may be regarded as sufficient for the description of the reconstruction). For example, for the 2×1 reconstruction the number of cells $m = 2$, whilst for the 2×4 reconstruction the corresponding number is $m = 8$.

As a result of the reconstruction, the bands of surface states are changed. As a rule, an unoccupied band tends to be 'repelled' from an occupied one (Fig. 14*c*) and their positions on the energy scale are altered (sometimes they move outside the limits of the forbidden band gap). Even greater changes are observed as a function of the energy of the quasi-momentum $\mathscr{E}_{\Delta,i}(\mathscr{K})$ in different bands (the subscript i indicates that the surface states belong to a particular band). As a rule, the region where this function is defined diminishes on reconstruction (for example, the Brillouin surface band decreases by a factor of 2 for the 2×1 reconstruction); there is a corresponding increase in the number of bands of surface states (Fig. 14*d*).

Under certain conditions, structures possessing only linear translational symmetry arise on the interface. the simplest examples may be the bands of the reconstruction dimers, the symmetry of which is disturbed in the direction perpendicular to the band or the polyatomic steps arising on the interface when the latter is a plane perpendicular to one of the crystallographic axes and is inclined at a low angle relative to the integral crystallographic plane. In this case, additional bands of surface states arise, for which the range of values of the quasi-momentum degenerates to a one-dimensional segment.

For the construction of a system of linear equations defining the energies of the surface states, the overlap integrals, found with the aid of the GPSE, are sufficient.

A surface with a complex shape. When partial symmetry is retained (reconstruction with a large cell, repeating corners, steps, etc.), the number of components of the vector $\vec{\Delta}$ and the range of values of i increase. The nature of the band structure remains the same as in Fig. 14*d* and the only difference is that new bands of surface states arise and hence the region where the functions $\mathscr{E}_{\Delta,i}(\mathscr{K})$ are defined becomes depleted (for certain values of i, the range of values of $\mathscr{K}$ may degenerate to a segment).

Further specification of the shape of the surface in an individual form leads to loss of symmetry. Together with bands of surface states, individual states appear (Fig. 14*e*), in which the range of values of $\mathscr{K}$ is zero-dimensional. These surface states are

localised in one or several cells; they are formed as a rule on individual (nonrepeating) pits, irregular hillocks, or even atoms. The decrease in symmetry is accompanied by an increase in the dimensionality of the vector $\vec{\Delta}$. When the surface has fully lost the two-dimensional translational symmetry, the dimensionality of $\vec{\Delta}$ is equal to three times the number of surface atoms.

In order to determine the electronic spectrum and the electronic surface states, it is necessary to solve a system comprising a larger number of equations than in solid state problems having three- or two-dimensional translational symmetry. The lack of symmetry in a surface with an individual shape makes it necessary to calculate a set of different overlap integrals and to solve systems of equations of an enormous dimensionality—this is in fact the main difficulty. In reality, only the GPSE in the form of Eqn (21) permits numerous valid solutions of this problem for a wide variety of configurations.[142,143] In addition, it is necessary to investigate the dependence of the reconstruction shifts on the nature of the assumptions made.

b. The model of the chemical modification of the surface

Fig. 15 illustrates schematically a block-diagram for the modelling of the chemical modification of the surface.[97,143]

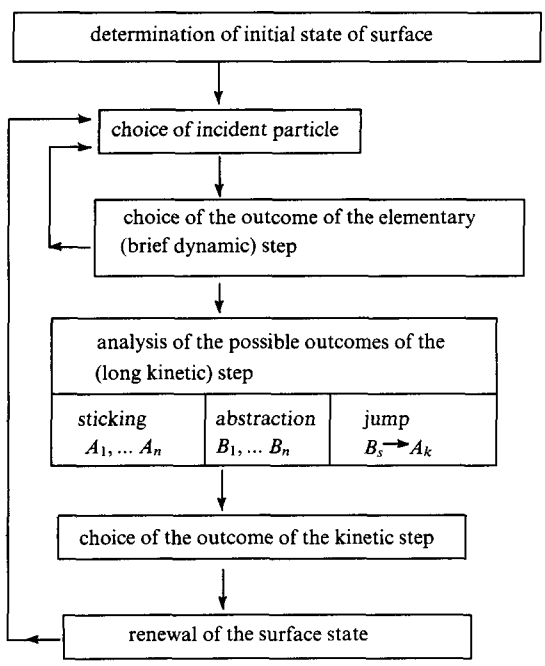


Figure 15. Block diagram of the modelling algorithm.

1. Initial state of the surface. The geometry of the near-surface atoms is specified by a three-dimensional Boolean matrix. Each lattice site is characterised by the numerals 1 or 0 depending on whether the site is occupied by an atom or not. The reconstruction and relaxation shifts of the atoms (the vector $\vec{\Delta}$) are calculated or those known beforehand are employed. The atoms are assumed to be stationary and their positions are averaged with respect to thermal motion. The spectrum and wave functions of the electronic surface states are calculated.

2. The choice of the incident particle. The number of the projection of the unit cell entered by the particle is selected. If the stream of particles has a nonuniform composition, then the kind of incident particle is selected.

3. The outcome of the elementary dynamic step. With the aid of the probabilities of elementary processes selected beforehand and averaged in one way or another, the specific outcome of a dynamic event is determined: sticking, dissociative sticking, etc. In the case of reflection the calculation has to be restarted again from block 2.

4. Analysis of the possible outcomes of the kinetic process. The sticking particle does not immediately occupy a stationary state. This process is fairly prolonged and its result (at least at nonzero temperatures) may not be unambiguous. The particle passes from one metastable state to another (if the activation energy is comparable to the temperature) in the search for the most stable state. We shall regard this process as kinetic and shall describe it statistically.

In the case of the deposition of particles, for example those of silicon, on the surface of a silicon crystal, all the vacancies A_i which the given adsorbed atom can fill are considered. The bond energy is calculated for each of them. This is done with the aid of the standard expression (20) for the surface + adsorbed atom system, the spectrum and wave functions of the surface states determined in the first stage of the algorithm being used for the surface, while the nondiagonal elements are adopted in the form of overlap integrals, which are estimated in accordance with the general GPSE rules.

In the vicinity of the incidence of the modifying particle, the possibility of the extraction of each surface atom B_i is considered in succession. The energies of such extraction are calculated (the procedure is in a certain sense the opposite of that mentioned above for the calculation of the bond energy). A procedure is specified for the removal from the surface of clusters of definite composition (for example, SiF_2 in the etching of silicon by fluorine-containing substances)

Furthermore, the possibility of the extraction of any of the surface atoms at the point B_s with its subsequent deposition at the point A_k, which describes surface diffusion, is considered. With the aid of the combination of the procedures classified previously, the activation energies for each of the possibilities and the extent to which they are energetically favourable are determined.

5. Selection of the outcome of the kinetic step. The result of the kinetic step arises statistically depending on the temperature of the surface and the energy changes in each of the alternative transitions.

6. The renewal of the state of the surface. In conformity with the results obtained in block 5, the Boolean matrix of the state is corrected, the construction shifts $\vec{\Delta}$ are redetermined, and the spectrum of the electronic surface states is found. The computation returns to block 2, after which a new particle is incident on the surface.

Measured quantities. Despite its apparent self-evident nature, the determination of the local surface level is not entirely unambiguous. Its position has been determined[97,143] on the basis of the condition that the number of atoms above the surface level is equal to the number of vacancies under it in the same column of atoms (a column of the Boolean matrix).

The average characteristics, the simplest of which is the average surface level and the rate of its change v, as well as the fractal dimensionality of the surface d and the dynamics of its change $d(t)$, are of principal interest. The quantities v, d, and $d(t)$ are found to depend only slightly on the method used to find the local surface level, which indicates that their determination is correct.

Furthermore, it is possible to determine the statistical properties of the surface—the scaling exponents α and β. A necessary condition for this is the possibility of modelling sections of the surface, the linear dimensions of which exceed L_c significantly.

The geometrical properties of the surface were considered above. Together with these, it is possible to determine the parameters characterising the chemical properties of the individual surface obtained in the computation. The algorithm makes it possible to calculate the energies of the unoccupied and occupied electronic surface states relative to the Fermi level and to model the possible overlap integrals of these states with the wave functions of the additional adsorbed atoms.

3. The surfaces of polymers

The differences between the structures and the electronic states of polyethylene molecules on the surface and in the bulk phase are not quite so great as, say, in silicon. In the modelling of the chemical modification of the surface by reactive incident particles, this makes it possible to disregard the surface state of the polymer and to employ the states of the molecules. Thus we do not differentiate between the modification of the units on the surface and the units in the succeeding layers to which the reactive particle can permeate by diffusion.

Extremely sophisticated computational methods have been developed in the theory of polymers. The GPSE method cannot compete with them as regards the accuracy of the determination of the structure and properties of specific molecules. However, this method permits estimates in fairly complex cases, in particular for large organic molecules, which can be regarded as a set of fragments the centres of which are tetravalent carbon atoms. In the consideration of covalent bonds between the atoms of Group IV elements, the simplicity and universality of the GPSE method have been manifested particularly clearly. We shall demonstrate this approach to the qualitative description of the chemical modification of polymers[142] in relation to polyethylene as an example.

a. The molecule

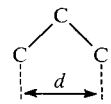
Polyethylene consists of macromolecules the structural unit of which is the $-CH_2-$ fragment. Since the pitch of the helix is significantly greater than the distance between these fragments, we shall consider it as a chain based on a zig-zag arrangement of carbon atoms. By virtue of the similarity of the energy of the *s* state of hydrogen and the average energy of the sp^3-hybridised state of carbon, a tetrahedral symmetry of the chemical bond is obtained for each carbon atom. In this approximation, the angles between the bonds in the $-CH_2-$ fragment of the polyethylene molecule are the same as in the CH_4 molecules or in the diamond crystal.

In considering the C–C bond (Fig. 16a), we can employ the same procedure as in the consideration of the chemical bonds in crystallised silicon (Fig. 13). The overlap integral between the orbitals of the nearest carbon atoms, calculated with the aid of the GPSE procedure, determine the bonding and antibonding states of the C–C bond [Eqn (22)], while the overlap integrals between the bonding and antibonding states of neighbouring units determine the width of the one-dimensional quasi-band.

The C–H bond can be considered similarly (Fig. 16*b*), but in this case the bonding and antibonding states in Eqn (23) are made up of the *s* orbital of hydrogen and the sp^3-orbital of carbon (approximation *IIa*). The smallness of the overlap integral between the two bonding (as well as antibonding) states adjoining a single carbon atom gives rise to some scatter of the latter as a function of the type of symmetry in relation to the transposition of the hydrogen atoms (approximation *IIb*). The width of the one-dimensional quasi-bands may be neglected for C–H bonds.

The complete scheme of the electronic states is presented in Fig. 16*c*.

For a rough test of our model, one can compare the form of the zig-zag with the real, experimental shape of the polyethylene molecule. The angle between two C–C bonds is tetrahedral and the length of the C–C bond obtained by the GPSE procedure is 1.54 Å; accordingly, the linear period of the molecule *d* is found to be 2.50 Å. The measured bond angle in the polyethylene molecule is 112° and the measured period is 2.55 Å, which are close to the calculated values (109° and 2.50 Å). This shows that the model which we have proposed describes the real molecule quite well.



b. Modification of the surface

In order that the metal atoms (M) should be able to modify polyethylene, it is necessary that the energies of the vacant states of the metal should be significantly higher than the energy of the antibonding orbital of the C–H bond. In this case, the valence electrons of the metal pass to the antibonding C–H orbitals (Fig. 16*c*). The presence of an electron in this orbital weakens the C–H bond, the hydrogen atom is split off, and the electron given up by the metal occupies an even more favourable position at the bonding level of the C–M bond formed.

The appearance of the metal on the surface of polyethylene decreases its permeability to gases. Firstly, the metal atoms are positively charged owing to the displacement of electrons towards carbon, which leads to their interaction with the induced dipole moments of the molecules of the permeating gases. Secondly, the residual partially unpaired valence electrons of the metal lead in some cases (for example on permeation of oxygen) to the formation of oxides which decrease the unoccupied gaps between the molecules. Thirdly, the metal atoms may cross-link the neighbouring polyethylene molecules.

We may note that the deposition of the metal on polyethylene presents certain difficulties. This problem has been studied experimentally, for example for magnesium.[144] It was noted that sticking becomes possible if polyethylene is first treated with a plasma or by ion bombardment. Novak et al.[144] did not explain this effect. The application of the GPSE method makes it possible to understand that in this type of treatment an electron is transferred from the bonding C–H state to the antibonding state and the mechanism under discussion ceases to operate immediately from the second stage, which does not require any additional assistance.

Thus, by virtue of its relative simplicity, the GPSE method makes it possible to model fairly complex processes which have not been investigated by other methods. We emphasise that the GPSE method can be applied in two stages of the investigation. With its aid, one models, firstly, the interaction of the incident particle with the surface and, secondly, the surface itself.

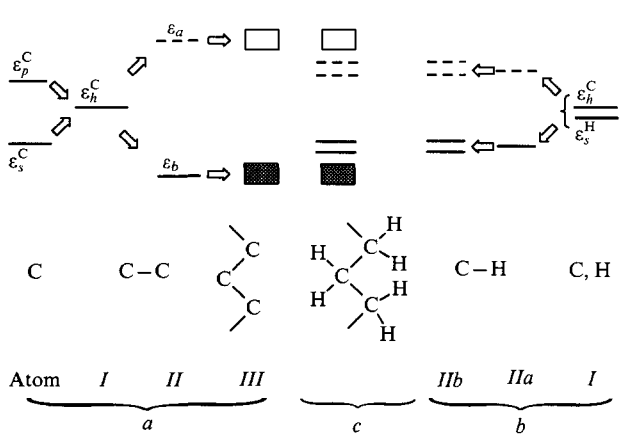


Figure 16. Construction of the energy diagram for the electronic states of a polymer molecule: (*a*) C–C bond; (*b*) C–H bond; (*c*) macromolecule.

XII. Results of the modelling of the modification of the surface

1. Continuous models

Apart from the competition between random deposition or etching (increase in the roughness of the surface) and diffusion (smoothing), which are common to the majority of such models, Karkar et al.[145] took into account also the competition within the $\hat{A}\{H(r,t)\}$ term between processes with different spatial locations.[129]

$$\frac{\partial H(r,t)}{\partial t} = \gamma\nabla^2 H(r,t) + \frac{\lambda}{2}[\nabla H(r,t)]^2 + \eta(r,t) \ .$$

The first term takes into account the revaporisation-condensation of the substance and hence the decrease in the surface area owing to the decrease in the height of hills and the filling of valleys. The second describes the growth of the surface in the direction of the local normal (which happens in the isotropic deposition of the modifying particles, i.e. at high pressures). The scaling exponents α and β proved to be independent of the numerical values of γ and λ: $\alpha = 0.38$ and $\beta = 0.24$.

Another smoothing mechanism—diffusion along the surface—has been considered by Wolf and Villain.[146] This process is characterised by a smaller scale than that considered by Kardar et al.[145] The equation for $H(r,t)$ was proposed in the following form:

$$\frac{\partial H(r,t)}{\partial t} = -\nu\nabla^4 H(r,t) + \eta(r,t) \ .$$

The values $\alpha = 1$ and $\beta = 1/4$ were found. A deficiency of the proposed operator $\hat{A}$ in this form is the failure to retain the surface diffusion flux. A nonlinear term was introduced to retain this flux.[147,148] In this case

$$\frac{\partial H(r,t)}{\partial t} = -\nu\nabla^4 H(r,t) + \lambda\nabla^2[\nabla H(r,t)]^2 + \eta(r,t) \ .$$

It has been shown[147] that for short times the first term predominates and the scaling exponents are close to those obtained by Wolf and Villain.[146] In the course of time, the second term becomes dominant and the scaling exponents approach $\alpha = 2/3$ and $\beta = 1/5$. It has been shown that allowance for nonlinearity in any form should decrease the scaling exponents.

Experimental values of the scaling exponents. A study has been made[149] of the deposition of copper chloride on the (111) surface of calcium fluoride by the method of molecular-beam epitaxy. The measured local static roughness index α proved to be 0.84 ± 0.05, which permitted the conclusion that the smoothing processes which accompanied the nonuniform deposition are much closer to surface diffusion[146] than to revaporisation.[145] The value of α found is somewhat lower than that determined by Kardar et al.,[145] which is evidence in support of the view that nonlinearity in the equation for $H(r,t)$ exerts an influence, but α is greater than in studies[147,148] involving a specific form of the nonlinear term ensuring the retention of the surface diffusion flux.

Iwamoto et al.[150] investigated the kinetics of the surface roughness in the electrodeposition of copper. The local roughness index, measured over small sections, proved to be identical, within the limits of the accuracy of measurement, with the index found by Tong et al.:[149] $\alpha = 0.87 \pm 0.05$. This confirms the conclusion[149] that surface diffusion predominates over revaporisation.

The results of averaging over large distances proved to be more unexpected. The measured dynamic exponent β proved to be 0.45 ± 0.05, which does not fit the concept that nonlinear terms exert an influence.[149] This has been attributed[150] to the effect of the electric field, which increases the vertical component of the growth of the surface, suppressing the lateral component.

2. Corrosion

A method has been proposed[151] for modelling corrosion within the framework of a two-dimensional cell model, only two parameters being employed: the passivation rate constant k_p and the depassivation rate constant k_d. The initial state is a two-dimensional rectangular grid (periodic boundary conditions are imposed along one of the coordinates) divided in such a way that the metal atoms are located at the nodes of one half-plane (capable of corroding) while particles inducing corrosion are at the nodes of the other half-plane. The interface is represented by passivating particles (oxide molecules adsorbed on the metal). Particles of a fourth kind can arise during corrosion: an inactive particle (a nonadsorbed molecule of the corrosion product, a neutral molecule, or an unoccupied node).

The process begins with spontaneous breakdown of the integrity of the interface. After a certain time δt, the probabilities of passivation (P_p) and depassivation (P_d) are established.

$$P_p = \delta t\, N_s k_p, \qquad P_d = \delta t\, N_p k_d \, .$$

In these expressions, N_s and N_p are the number of unprotected metal atoms (capable of coming into contact with the corroding particles) and the number of protected metal atoms (on which oxides are adsorbed) respectively. During corrosion, each lattice site can be occupied by a particle of one of the four kinds indicated above.

The cases of small scales and times (specimen length equivalent to 128 particles) and large scales and times (specimen length equivalent to 8192 particles) were considered. The first case (to some extent arbitrary owing to its two-dimensionality) corresponds to the condition $L_c \ll L$, whilst the second corresponds to $L_c \gg L$ in Eqn (19). The methods used to represent the results are also different.

In the first case, virtually nothing happens for large values of k_p—the cavity formed passivates itself. For low values of both k_p and k_d, the cavities grow in a stable manner and have an approximately hemispherical shape and relatively smooth edges. For large values of k_d, the structure of the interface becomes increasingly irregular. The fractal dimensionality of the interface increases with increase in the ratio k_d/k_p.

In the second case, the time variations of the corrosion current yields more information. Such variations have as a rule a typical pulsed form with a characteristic sharp initial rise corresponding to the onset of the formation of the cavity. The rises on the curve indicate the onset of the formation of new corrosion centres in the cavity. It has been noted that minor corrosion current pulses and shorter intervals between the pulses correspond to large values of k_p and k_d respectively. A universal empirical time dependence of the average corrosion current has been proposed:

$$I(t) \sim \frac{f(t/t^*)}{\ln t} \ ,$$

where the function $f(x)$ is constant for small values of x, decreasing rapidly for high values of x. The parameter t^* is related to the passivation rate constant by the expression

$$k_p^2 t^* \ln t^* \sim \text{const.}$$

Despite its approximate nature, this model describes correctly many aspects of the phenomenon and the principal process. Agreement has been found with the results of the continuous modelling of the morphology of the surface. The parameters k_d and k_p apparently characterise the universal corrosion mechanisms for different solid and liquid metals under the influence of various corrosion factors. Depending on their magnitude, the model describes both stable and unstable growth of the corrosion cavities.

3. Deposition and etching

The modelling of the chemical modification of the surface carried out [97, 143] with the aid of the algorithm described in Section X may be regarded as a demonstration. Many processes determined by surface states have not so far been modelled. At the same time modelling even at this level makes it possible to describe the selective filling of vacancies with the largest number of possible bonds (or the elimination of the least bound atoms) and to discover the characteristic features of the crystal lattice shape formation. It permits the description of different modification regimes: deposition, polishing, and etching, and permits a comparison of the qualitative aspects of the morphology with certain models by using literature data.

The chemical modification of the crystal surface of silicon with the base perpendicular to the [001] direction has been modelled. The initial surface (Fig. 17) was specified in a form such that the evolution of both smooth and sharp changes in relief could be observed. Streams of particles characterised by a conventional chemical energy E were considered for the modelling of the possible regime. Numerical experiments with various values of this quantity revealed three characteristic regimes: the changes in the form of the surface in all these regimes after the deposition of 20 000, 80 000, and 200 000 particles on the support are illustrated in Figs. 18*a*, 18*b*, and 18*c*.

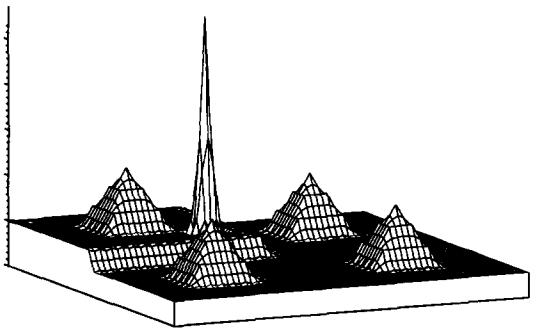


Figure 17. Initial relief of the modelled surface. The size of the section is 123 × 123 Å.

Deposition. In the first regime, particles with a low value of E fall on the support. There is then a certain number of particles capable of rupturing one and two bonds and very few particles capable of rupturing three bonds; there are virtually no particles which can rupture four bonds. If surface atoms with free bonds fall within the range of the influence of the valence electrons of the incident particles, new bonds may be formed. The effect of particles with such energy leads to a gradual growth of the crystalline layer, whereupon the form of the surface is approximately retained, being distorted mainly as a result of nonuniform sticking. Particles are eliminated rarely, such elimination being most notably manifested in the smoothing of sharp variations of the relief, in which the particles have the smallest number of bonds.

In the initial stage, the modification of the surface is close to that described by the simplest random deposition model.[117] It may be assumed that in the given instance the quantity L_c is fairly small and the roughness of the film is approximately proportional to the square root of the change in the height of the support. In the course of time (with increase in the number of incident particles), features characteristic of the ballistic deposition model appear [120–122] and projections and holes arise. The quantity $L_c \sim t^{\beta/\alpha}$ also increases and exceeds the size of the modelled crystal specimen. The dependence of the thickness of the film not only on the height of the support but also on its linear dimensions also begins to correspond to a power function. The fractal dimensionality of the surface formed increases. It may be expected that it tends to a definite limit with increase in the number of deposited particles.

Polishing. When particles with higher values of E are deposited, the situation changes radically. In this regime, almost all the deposited particles are capable of breaking one bond, quite a few particles are capable of breaking two and three bonds, and there are also particles able to break four bonds. The quantity E is

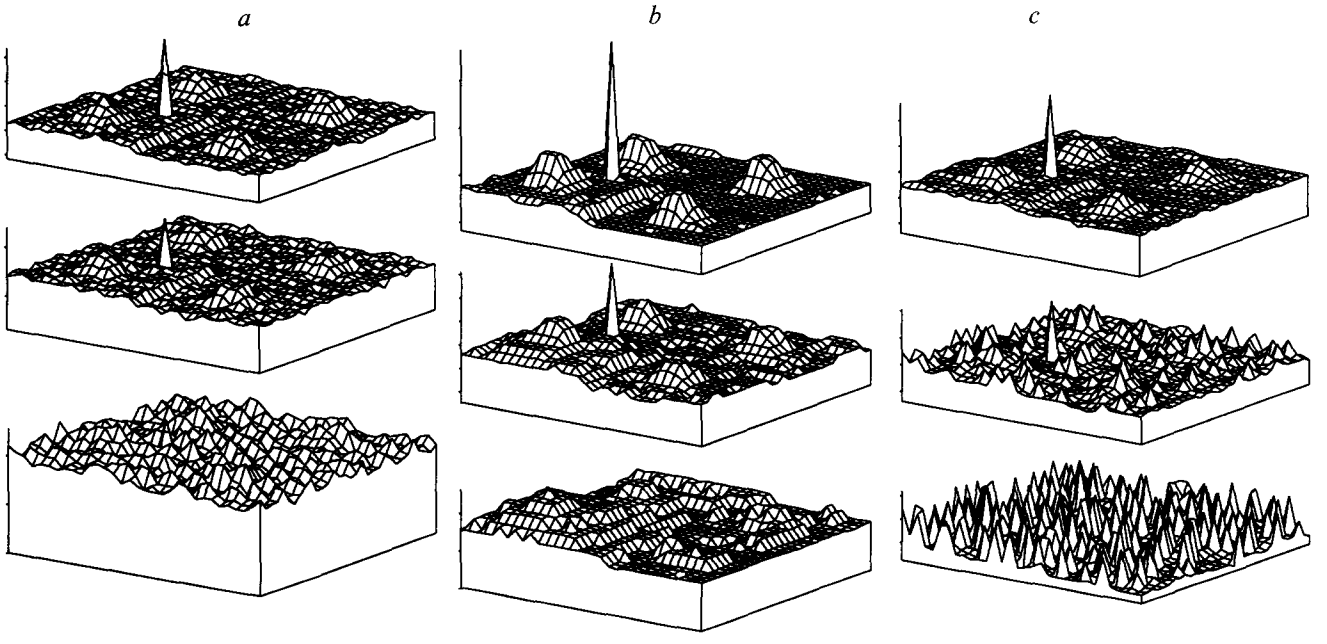


Figure 18. Modification of the surface in different regimes: (*a*) deposition; (*b*) polishing; (*c*) etching. The successive diagrams (from top to bottom) correspond to the deposition of 20 000, 80 000, and 200 000 particles.

selected so that the probability of rupture of the existing bonds corresponds to the probability of the formation of new ones. In the course of time, the surface relief becomes increasingly even. Projections are disrupted (the disruption of sharp ones is particularly rapid), but the average height of the support does not increase. The description of the surface modification processes under the influence of particles with such energy no longer corresponds to the models.[117,120] These processes are closer to those which may be described in terms of the statistical terraces model[121,122] and other models[123] describing the dynamics of the variation of formations with dimensionalities 1 or 2.

Etching. The situation again changes for a stream of particles with even higher values of E. In this regime, the majority of the particles have a chemical energy sufficient for the dissociation of three bonds and an appreciable number of particles are capable of rupturing all four bonds. The probability of the sticking of such particles to the surface is low and that of the dislodgment of crystal atoms is high, so that the thickness of the film diminishes. The initial form of the surface is gradually forgotten and is transformed into a very random landscape in the course of time. The fractal dimensionality of the modified surface increases as in the case of particles with low values of E (by analogy with this case, one may expect that the dimensionality tends to a limit with increase in the number of deposited particles). In a certain sense, the random and ballistic etching models, and not deposition models as described in the above investigations,[117,120-122] operate.

Within the framework of the calculations carried out, particles with low values of E play the role of silicon atoms in the absence of oxidising particles, while those with large values of E play the role of atoms (or molecules) of fluorine or other oxidising substances. This analogy, like that with cold or very hot particles, is extremely arbitrary. Effects such as etching after the formation of a monolayer cannot be modelled either.

Thus, within the framework of one model,[97,143] it has been possible to obtain different regimes in the modification of the surface and in the alteration of its morphology (Fig. 19), which had previously been described by means of various approaches.

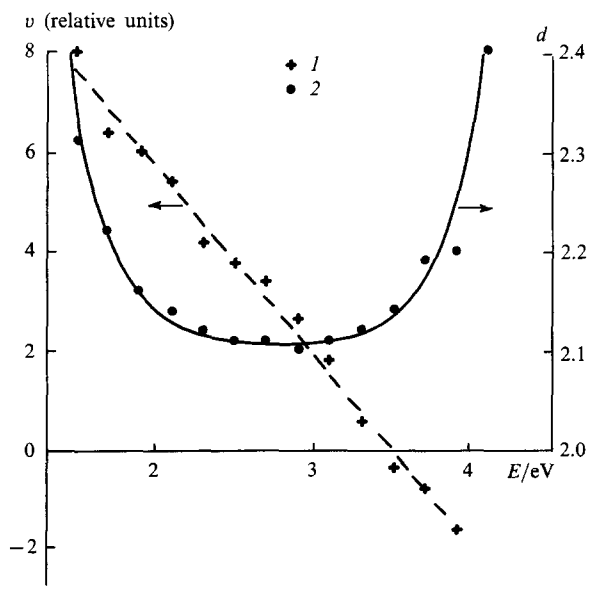


Figure 19. Rate of modification of the surface υ and the fractal dimensionality d as functions of the conventional chemical energy E of the incident atoms. The dashed line was obtained by fitting $\upsilon \sim (3.5 - E)$ and the continuous line was obtained by fitting $-d(E) = 2.1 + 0.1(E - 2.8)^4$.

The rate of change of the average level of the modified surface depends linearly on the quantity E, whereas the fractal dimensionality of the final surface is satisfactorily represented by a fourth degree parabola.

The existence of these relations throws light on the significance of the quantity E, which has hitherto played the role of a model parameter. Its linear relation with the rate of change of the average level of the surface makes it possible to employ E as a unique quantitative parameter (instead of a whole set of concentrations of various particles, their temperatures, etc.) characterising the effectiveness of the chemical action of a gas-plasma stream on the surface.

The minimum in the fractal dimensionality of the final surface is correlated with the passage of the rate of change of the level through zero. We may note that in a real situation the conclusion that the minimum in the fractal dimensionality of the final surface is related to the constancy of the thickness of the support may prove not to be universal. Thus an important factor in the description of surface modification processes may prove to be the presence of several kinds of incident particles with different values of E—some particles may etch the surface, whilst others are deposited. In different situations, the smoothness, the purity of the composition and the rate of change of the thickness of the support may be ensured by different groups of particles.

4. Problems with several time and length scales

As mentioned in Section VIII, the dynamic and probability methods have different applications, which supplement one another. This makes it useful to achieve their joint employment. Both these and other methods have extremely different versions and for this reason the procedures for combining them are also quite diverse.

Thermal desorption. The approaches combining the MMD and the transition state theory (the probability approach) make it possible to investigate rare events. Thus a study has been made[151] of the thermal desorption of a Xe atom from a Pt(111) surface. With the aid of the transition state theory,[152] the process probability being sought is represented by 'equilibrium' and 'dynamic' cofactors. The latter is expressed in terms of the sticking coefficient of the atom incident on the surface and is calculated by the MD method. The equilibrium factor can be determined by various methods, both statistical and dynamic. In both cases the application of special procedures is needed to improve the statistics in the 'bottleneck' within the phase space, the crossing of which by the phase trajectory is unlikely, but this 'bottleneck' determines the thermal desorption section. Several such procedures (stochastic dynamics and the 'boxes' and compensating potential methods) have been described[151] for the dynamic version of the calculation of the equilibrium cofactor.

A similar approach has been used[153] to calculate the rate of evaporation of a 14-atom cluster at low temperatures.

Diffusion of adsorbed atoms. Among the most recent studies, those[154,155] in which the diffusion of adsorbed Si atoms on the Si(100)-(2 × 1) surface and of Ge atoms on the Ge(100)-(2 × 1) surface as well as the dynamics of the adsorbed Si atom and the mechanism of the epitaxial growth of the Si(100)-(2 × 1) surface with a terrace are the most characteristic.

Such processes are characterised by two time scales: for short times, the atom captured by the surface seeks a stable adsorption site, while for long times the atom diffuses by jumps from one adsorption site to another and the scale is determined by the residence time of the atom at the sites. The calculation is therefore carried out in two stages, in each of which different methods are applied.

In the first stage, the adsorption energy profile was determined by the MD method along the surface modelled by several layers of mobile particles. The Tersoff potential was used.[23] The Si

atom was projected onto the Si surface and was allowed to select a sticking point (long arrest at a particular site). The surface was then gradually brought to zero temperature and its energy was calculated. The energy difference between the equilibrium surface and the surface with an adsorbed atom at the given point was assumed to be the adsorption energy. Such depositions were repeated many times at different points on the surface, which made it possible to construct a detailed adsorption energy profile.

The activation energies for the jump to a neighbouring adsorption site and the vibration frequencies of the adsorbed atoms at different sites were determined from the calculated profile and were subsequently used in the second stage of the calculation, where a probability method was employed. The Si atom was placed at random at a certain point on the calculated surface $E_a(x, y)$, where E_a is the adsorption energy and x and y are the coordinates along the surface. The probability P_{ij} of a jump from the adsorption site i to a nieghbouring site j was then selected stochastically. According to the transition state theory, $P_{ij} = \upsilon_{ij} \exp(E_{ij}/kT)$, where υ_{ij} is the vibration frequency of the adsorbed atom at i in the direction of the transition to j and E_{ij} is the activation energy for the transition.

The results[154] showed that the adsorbed atoms diffuse predominantly in the direction along rows of dimers, which has in fact been observed experimentally.

In epitaxy on a stepped surface,[155] the procedure is similar. The diffusion of the given adsorbed atom is terminated artificially at the instant when the next adsorbed atom appears on the surface (in accordance with the rate of deposition).

Condensation of supersaturated vapour. A model of the initial stage in the formation of clusters in supersaturated vapour has been considered.[156,157] The problem involves processes differing in both time and length scales: elementary steps involving sticking and evaporation and the kinetics of the growth of the size and number of drop nuclei. Processes of the first type are dynamic, while those of the second are statistical. The system of kinetic equations for the variation of the concentrations of the atoms in the clusters in a rarefied gas is used as the initial system. These equations include the rate of formation of dimers, the rate of sticking of atoms to the clusters and of the clusters to one another, and the rate of evaporation of atoms from the clusters and of the break up of the clusters. The problem is divided into two stages. In the first stage, the rates of elementary processes are calculated by the MD method, whilst in the second the kinetic equations are integrated numerically. This approach has been used in a calculation for the condensation of metals behind the shock wave front propagated in an inert gas in the presence of different amounts of an added volatile compound of the metal[156] and for the condensation of argon in a hypersonic stream.[157]

Deposition. As an example of the possible application of the ideas outlined in Section XI, we shall consider the deposition of gold on a silver support at room temperature. This problem has been modelled[158] by the MD method. Two assumptions were made. Firstly, the rate of deposition (one gold atom during a period $\lesssim 1$ ns on an area comprising 6×8 silver atoms) was assumed to be greater by many orders of magnitude than in the real deposition. Secondly, in order to compensate for such a high rate, an annealing procedure was introduced: each Au atom fell on a surface heated to 810 K, which was cooled after relaxation. This simulated the conditions where after each elementary step the surface returned to the equilibrium state. In particular, the gold atoms diffused into the first and second layers of silver atoms and the silver atoms were displaced to the state of adsorbed atoms.

In a real process, there are two markedly different time scales. With the aid of the above procedures, the authors[158] shortened the deposition time to values close to the time of an elementary step. The problem can be solved also by a different procedure after dividing it into two stages. In the first stage, the elementary steps modelled by the MD method are differentiated: the incidence of a gold atom on a clean silver surface and on sections of the silver surface with one, two, three, and more gold atoms in characteristic positions. Together with sticking processes, the subsequent diffusion is modelled and the energies of the potential barriers and the temperature variations of the pre-exponential factors are determined and extrapolated to low temperatures.

In the second stage, the deposition process at the required temperature is modelled with the aid of probability approaches using the information already obtained about the elementary steps. This approach would make it possible to expand significantly the temporal and spatial framework of the problem compared with those considered in the study of Haftel et al.[158] and also to turn attention to cases where there is insufficient time for the attainment of equilibrium between successive incidences of the atoms. In order to determine the extent to which the state of equilibrium is attained in the given processes, it is necessary to include in the consideration surface phonons and other types of surface excitation arising during the incidence of the particles.

5. Certain future tasks

Without claiming to quote a complete list, we shall present certain examples from the physics and chemistry of surfaces which may become the field of the active application of molecular modelling methods.

Elementary chemical processes. Scanning tunnel microscopy and certain other methods have made it possible to proceed to the study of the structure of the surface and the processes occurring on it at the level of individual molecules or atoms, for example the dynamics of the dissociative chemisorption of $Cl_2/Si(111)-(2 \times 1)$,[159] the dynamics of the deposition of an individual atom (iridium) on the iridium surface (steps and clusters),[160] the diffusion of $Si(001)-(2 \times 1)$ vacancies,[161] etc. Such studies naturally stimulate the development of molecular modelling methods.

Heterogeneous catalysis. The phenomena in heterogeneous catalysis are based on the change of the chemical properties of the atoms and molecules which have formed chemical bonds with the surface. For example,[143] data on the decrease in the dissociation energy of the O_2^- molecular ion on the surfaces of transition metals by an order of magnitude (under certain conditions by two orders of magnitude)[162] and on the increase in the interatomic distance[163] have been quoted to illustrate the enhancement of the oxidative properties of an adsorbed oxygen molecule. Quali-tatively, this phenomenon can be understood within the framework of the idea concerning the chemical properties of a surface described in Section X. This refers also to the results of a study[164] where an increase in the Fermi level as a result of the additional filling of the surface states by the valence electrons of the adsorbed sodium atoms and its decrease as a result of the reverse process in the adsorption of sulfur atoms were described. For a quantitative description and development of methods for controlling catalytic properties, molecular modelling is required.

Reconstruction dynamics. The calculation of the surface reconstruction time is an interesting and hitherto unsolved problem. Here there are no differentiated atoms and it is not always evident how many atoms should be considered in the modelling of a nonstationary quantum process. There remain many problems even for the stationary case of a thoroughly investigated surface such as $Si(001)-(2 \times 1)$.[165]

Nonequilibrium materials. The study of the structure of a surface with different ratios for the rate of reconstruction and the rate of deposition may lead to the explanation of the difference between the lattice constants of the ultradisperse powders obtained by the plasmochemical method[166] and its value for a massive specimen.

Multilevel molecular modelling makes it possible to understand the properties of nonequilibrium crystals and facilitates the search for ways of synthesising them.

Modification of the surface. The structure of the surface and the dynamics of its variation have become the object of experimental studies at the molecular level, in particular by means of tunnel microscopes.[167–169] The effect involving the appearance of instability in the form of the surface in molecular-beam epitaxy as a function of changes in the deposition regime has been observed.[167,168] Modelling demonstrated its usefulness even in the simplest geometric version.

Multilevel modelling. The problem is formulated so that: all the levels into which the problem is divided (elementary steps, collective processes, macroscopic description, etc.) are discovered; descriptive procedures for each level are selected; the channels for the transmission of information between the levels (initial data, parameters, initial and boundary conditions etc.) are established; the required level of accuracy of the final result is specified in the scheme, establishing thereby the required accuracy at each level or, conversely, the attainable accuracy of the final result is determined on the basis of the worst current accuracy for one of the levels.

In Dodson's review,[4] it is concluded that, because of the abundance of unelucidated questions, the molecular modelling methods still remain the objects of study and not a means of carrying out studies. The authors of the present review attempted to show how, by combining the dynamic and probability modelling procedures, it is possible to convert them into a means whereby research can be carried out. The choice of modelling problems is determined by physical effects, applied purposes, and the possibility of comparison with experiment.

This review has been written with the financial support of the Russian Fundamental Research Fund (Project 94-03-08069).

References

1. J C Tully, in *Many Body Phenomena at Surfaces* (Eds D Langreth, H Suhl) (New York: Academic Press, 1984) p. 377
2. F F Abraham, in *Molecular-Dynamics Simulation of Statistical-Mechanics Systems (Proceedings of the International School of Physics "Enrico Fermi")* (Eds G Ciccotti, W G Hoover) (Amsterdam: North-Holland, 1986) p. 130
3. V Borotolani, N H March, M P Tosi (Eds) *Interaction of Atoms and Molecules with Solid Surfaces* (New York: Plenum, 1990)
4. B W Dodson *Crit. Rev. Solid State Mater. Sci.* **16** 115 (1990)
5. J C Tully *J. Chem. Phys.* **93** 1061 (1990)
6. W Steele *Chem. Rev.* **93** 2355 (1993)
7. A A Valuev, G E Norman, V Yu Podlipchuk, in *Matematicheskoe Modelirovanie. Fiziko-Khimicheskie Protsessy* (Mathematical Modelling. Physicochemical Processes) (Ed. A A Samarskii, N N Kalitkin) (Moscow: Nauka, 1989) p. 5
8. G E Norman, V Yu Podlipchuk, A A Valuev *J. Moscow Phys. Soc.* **2** 7 (1992)
9. G E Norman, V Yu Podlipchuk, A A Valuev *Mol. Simul.* **9** 417 (1993)
10. A S Kaklyugin, G E Norman, in *Termodinamika Neobratimykh Protsessov* (Thermodynamics of Irreversible Processes) (Ed. A I Lopushanskaya) (Moscow: Nauka, 1987) p. 5
11. A S Kaklyugin, G E Norman *J. Moscow Phys. Soc.* **5** (1995) (in the press)
12. V M Zamalin, G E Norman, V S Filinov *Metod Monte-Karlo v Statisticheskoi Fizike* (The Monte Carlo Method in Statistical Physics) (Moscow: Nauka, 1977)
13. K Binder, D W Heerman *Monte Carlo Simulation in Statistical Physics: an Introduction* (Berlin: Springer, 1988)
14. W Harrison *Electronic Structure and the Properties of Solids* (San-Francisco: Freeman, 1980) (Translated into Russian; Moscow: Mir, 1983)
15. M P Allen, D J Tildesley (Eds) *Computer Simulation of Liquids* (Oxford: Clarendon Press, 1987)
16. J M Haile *Molecular Dynamics Simulation: Elementary Methods* (New York: Wiley, 1992)
17. F F Abraham *Rep. Prog. Phys.* **45** 1113 (1982)
18. D J Evans *Phys. Rep.* **1** 297 (1984)
19. M S Daw, M I Baskes *Phys. Rev. B* **29** 6443 (1984)
20. F H Stillinger, T A Weber *Phys. Rev. B* **31** 5262 (1985)
21. J Tersoff *Phys. Rev. Lett.* **56** 632 (1986)
22. J Tersoff *Phys. Rev. B* **37** 6991 (1988)
23. J Tersoff *Phys. Rev. B* **38** 9902 (1988)
24. J Tersoff *Phys. Rev. B* **39** 5566 (1989)
25. R Biswas, D R Hamann *Phys. Rev. B* **36** 6434 (1987)
26. J R Chelikowskii, J P Phillips *Phys. Rev. B* **41** 5735 (1990)
27. D Brenner, B Garrisson *Phys. Rev. B* **34** 1304 (1986)
28. E Kaxiras, K C Pandey *Phys. Rev. B* **38** 12736 (1988)
29. E Pearson, T Takai, T Halicioglu, W A Tiller *J. Cryst. Growth* **70** 33 (1984)
30. B W Dodson *Phys. Rev. B* **35** 2795 (1987)
31. D Mistriotis, N Flytzanis, S C Farantos *Phys. Rev. B* **39** 1212 (1989)
32. E Khor, S Das Sarma *Phys. Rev. B* **38** 3318 (1988)
33. B C Belding, H C Andersen *Phys. Rev. B* **41** 10568 (1990)
34. A P Sutton, J Chen *Philos. Mag. Lett.* **61** 139 (1990)
35. M I Baskes, J S Nelson, A F Wright *Phys. Rev. B* **40** 6085 (1989)
36. H Baalamane, T Halicioglu, W A Tiller *Phys. Rev. B* **46** 2250 (1992)
37. X-P Li, G Chen, P B Allen, J Q Broughton *Phys. Rev. B* **38** 3331 (1988)
38. E Khor, S Das Sarma *Phys. Rev. B* **36** 7733 (1987)
39. J Q Broughton, X-P Li *Phys. Rev. B* **35** 9120 (1987)
40. J S Kallman, W G Hoover, C G Hoover, A J De Groort, S M Lee, F Wooten *Phys. Rev. B* **47** 7705 (1993)
41. A A Valuev *Zh. Fiz. Khim.* **69** 271 (1995)
42. M D Kluge, J R Ray *Phys. Rev. B* **39** 1738 (1989)
43. K Tsumuraya, K Ishibasi *Phys. Rev. B* **47** 8552 (1993)
44. F H Stillinger, T A Weber *J. Chem. Phys.* **88** 5123 (1988)
45. P C Weakliem, E A Carter *J. Chem. Phys.* **98** 737 (1993)
46. W Yin, P Vashinta, R K Kaliza *Phys. Rev. B* **48** 9359 (1993)
47. D H Robertson, D W Brenner, C T White *Phys. Rev. Lett.* **67** 3132 (1991)
48. M I Baskes *Phys. Rev. B* **46** 2727 (1992)
49. R Car, M Parrinello *Phys. Rev. Lett.* **55** 2471 (1985)
50. C Z Wang, C T Chan, K M Ho *Phys. Rev. B* **39** 8586 (1989)
51. F S Khan, J Q Broughton *Phys. Rev. B* **39** 3688 (1989)
52. D K Remler, P A Madden *Mol. Phys.* **70** 921 (1990)
53. M T Yin, M L Cohen *Phys. Rev. B* **26** 3259 (1982)
54. I Stich, R Car, M Parrinello *Phys. Rev. B* **44** 4262 (1991)
55. P E Bloch, M Parrinello *Phys. Rev. B* **45** 9413 (1992)
56. F Buda, G L Chiarotti, R Car, M Parrinello *Phys. Rev. Lett.* **63** 294 (1989)
57. R Car, M Parrinello *Phys. Rev. Lett.* **60** 204 (1988)
58. I Stich, R Car, M Parrinello *Phys. Rev. Lett.* **63** 224 (1989)
59. J Galli, R M Martin, R Car, M Parrinello *Chem. Phys. Lett.* **139** 540 (1989)
60. J Galli, R M Martin, R Car, M Parrinello *Phys. Rev. Lett.* **63** 988 (1989)
61. G Kresse, J Hafner *Phys. Rev. B* **47** 557 (1993)
62. Ch Lee, D Vanderbilt, K Laasonen, R Car, M Parrinello *Phys. Rev. B* **47** 4863 (1993)
63. K Laasonen, M Sprik, M Parrinello, R Car *J. Chem. Phys.* **99** 9080 (1993)
64. D Tománek, M A Schlüter *Phys. Rev. B* **36** 1208 (1987)
65. D J Chadi *Phys. Rev. B* **29** 785 (1984)
66. C Z Wang, C T Chan, K M Ho *Phys. Rev. B* **40** 3390 (1989)
67. V I Gavrilenko *Phys. Rev. B* **47** 9385 1993
68. J L Mercer, M Y Chou *Phys. Rev. B* **47** 9385 (1993)
69. J L Mercer, M Y Chou *Phys. Rev. B* **48** 5374 (1993)
70. P C Weakliem, E A Carter *J. Chem. Phys.* **96** 3240 (1992)
71. P Boguslawski, Q-M Zhang, Z Zhang, J Bernholc *Phys. Rev. Lett.* **72** 3694 (1994)
72. C R Arumainayagam, R J Madix, M C McMaster, V M Suzava, J C Tully *Surf. Sci.* **226** 180 (1990)
73. B Rise, L Raff, D Thompson *Surf. Sci.* **198** 360 (1988)

74. Z A Insepov, A M Zhankadamova *Z. Phys. D, At. Mol. Clusters* **20** 145 (1991)
75. R M Logan, R E Stickney *J. Chem. Phys.* **44** 195 (1966)
76. B Jackson *J. Chem. Phys.* **98** 9905 (1993)
77. G L Keldsen, J B Nicholas, K A Carrado, R E Winans *J. Phys. Chem.* **98** 279 (1994)
78. S V Teplov, V V Zastavnjuk, V Bykov, J W Rabalais *Surf. Sci.* **310** 436 (1994)
79. K D Shiang *J. Chem. Phys.* **99** 9994 (1993)
80. K D Dobbs, D J Doren *J. Chem. Phys.* **99** 10041 (1993)
81. L Wang, Q Ge, G D Billing *Surf. Sci. Lett.* **304** L413 (1994)
82. C Engdahl, G Wahnström *Surf. Sci.* **312** 429 (1994)
83. M G Lagally *Phys. Today* (11) 24 (1993)
84. C Carraro, B Q Chen, S Schramm, S E Koonin *Phys. Rev. A* **42** 1379 (1990)
85. S Valkealahti, M Manninen, E Hammaren *Z. Phys. D, At. Mol. Clusters* **22** 547 (1992)
86. M H Shapiro, T A Tombrello *Phys. Rev. Lett.* **68** 1613 (1992)
87. I Kwon, R Biswas, G S Green, C M Soukoulis *Phys. Rev. B* **41** 3678 (1990)
88. M Schneider, I K Schuller, A Rahman *Phys. Rev. B* **36** 1340 (1987)
89. H Hsieh, R S Averback, H Sellers, C P Flynn *Phys. Rev. B* **45** 4417 (1992)
90. G Betz, R Kirshner, W Husinsky, H M Urbassek, F Rüdenauer *Radiation Eff. Defects Solids* **130–131** 251 (1994)
91. Z A Insepov, M Sosnovski, G H Takagka, I Yamada, in *Proceedings of the International Conference of Materials Research Societies, Boston, USA, 1993* p. 21
92. J A Nieminen, T Ala-Nissila *Phys. Rev. E* **49** 4248 (1994)
93. I Benjamin, M Wilson, A Pohorille *J. Chem. Phys.* **100** 6500 (1994)
94. P Ahlström, H J C Berendsen *J. Phys. Chem.* **97** 13691 (1993)
95. A A Gusev, U W Suter *J. Chem. Phys.* **99** 2228 (1993)
96. L A Carter, S Khodabandeh, P C Weakliem, E A Carter *J. Chem. Phys.* **100** 2275 (1994)
97. A S Kaklygin, G E Norman, V Yu Podlipchuk, B B Slavin, P I Sopin, A A Valuev *J. Moscow Phys. Soc.* **3** 127 (1993)
98. V J Barclay, D V Jack, J C Polanyi, Y Zeiri *J. Phys. Chem.* **97** 12541 (1993)
99. E E Nikitin *Teoriya Elementarnykh Atomno–Molekulyarnykh Protsessov v Gazakh* (Theory of Elementary Atomic–Molecular Processes in Gases) (Moscow: Khimiya, 1970)
100. H Gai, G A Voth *J. Chem. Phys.* **101** 1734 (1994)
101. D A Gibson, E A Carter *J. Phys. Chem.* **97** 13429 (1993)
102. M E Tuckerman, M Parrinello *J. Chem. Phys.* **101** 1302 (1994)
103. C S Carmer, B Weiner, M Frenklach *J. Chem. Phys.* **99** 1356 (1993)
104. T H Murphey, P J Rossky *J. Chem. Phys.* **99** 515 (1993)
105. E Keszei, S Nagy, T H Murphey, P J Rossky *J. Chem. Phys.* **99** 2004 (1993)
106. F Webster, E T Wang, P J Rossky, R A Friesner *J. Chem. Phys.* **100** 4835 (1994)
107. C Engdahl, U Nielsen *J. Chem. Phys.* **98** 4243 (1993)
108. A P J Jansen *J. Chem. Phys.* **99** 4055 (1993)
109. G Mills, H Jònsson *Phys. Rev. Lett.* **72** 1124 (1994)
110. W T Pollard, R A Friessner *J. Chem. Phys.* **100** 5054 (1994)
111. G A Voth, D Chandler, W H Miller *J. Chem. Phys.* **91** 7749 (1989)
112. V Yu Podlipchuk *Teor. Mat. Fiz.* **82** 145 (1990)
113. V Yu Podlipchuk *J. Moscow Phys. Soc.* **3** 37 1993
114. V S Filinov *Dokl. Akad. Nauk* (1995) (in the press)
115. S Wolfram *Rev. Mod. Phys.* **55** 601 (1983)
116. Yu K Tovbin *Prog. Surf. Sci.* **34** 1 (1990)
117. J D Weeks, G H Gilmer, K A Jackson *J. Chem. Phys.* **65** 712 (1976)
118. P Meakin *Crit. Rev. Solid State Mater. Sci.* **13** 143 (1988)
119. P Meakin, R Jullien, in *Modelling of Optical Thin Films (Proc. SPIE)* (Ed. M R Jacobson) 1988, p. 821
120. C S Lent, P I Cohen *Surf. Sci.* **139** 121 (1984)
121. J M Pimbley, T-M Lu *J. Appl. Phys.* **55** 182 (1984)
122. J M Pimbley, T-M Lu *J. Appl. Phys.* **57** 1121 (1985)
123. E Chason, J Y Tsao *Surf. Sci.* **234** 361 (1990)
124. B D Zubashevsky, V Privman, S C Roy *Phys. Rev. E* **47** 48 (1993)
125. J G Amar, F Family *Phys. Rev. E* **47** 1595 (1993)
126. D D Vvedensky, A Zangwill, C N Luse, M R Wilby *Phys. Rev. E* **48** 852 (1993)
127. I K Marmorkos, S Das Sharma *Surf. Sci. Lett.* **237** L411 (1990)
128. M Tomášek, Š Pick, G V Gadiyak, Yu N Morokov *Phys. Status Solidi B* **156** 243 (1989)
129. C Herring *J. Appl. Phys.* **21** 301 (1950)
130. F Family, T J Vicsek *Physica A* **18** L75 (1985)
131. F Family, T J Vicsek *Dynamics of Fractal Surfaces* (Singapore: World Scientific, 1991)
132. T J Vicsek *Fractal Growth Phenomena* (Hong Kong: World Scientific. 1992)
133. D J Chadi *Ultramicroscopy* **31** 1 (1989)
134. P V Smith, A Wander *Surf. Sci. Lett.* **219** 77 (1989)
135. X M Zheng, P L Cao *Surf. Sci. Lett.* **219** L543 (1989)
136. J E Northrup, M S Hybertsen, G Louie *Phys. Rev. Lett.* **66** 500 (1991)
137. T Yamaduchi, N Fujima *J. Phys. Soc. Jpn.* **60** 1028 (1991)
138. L V Keldysh *Priroda* (9) 17 (1985)
139. F I Dalidchik, S A Kovalevskii, N N Kolchenko, B R Shub *Pis'ma Zh. Eksp. Teor. Fiz.* **58** 511 (1993)
140. F I Dalidchik, M V Grishin, S A Kovalevskii, N N Kolchenko, B R Shub *Surf. Sci.* **316** 198 (1994)
141. F I Dalidchik, M V Grishin, S A Kovalevskii, N N Kolchenko, B R Shub, A I Volkov *J. Moscow Phys. Soc.* **3** 127 (1993)
142. A S Kaklyugin, in *Materialy VI Mezhdunar. Shkoly-Simpoziuma po Khimicheskoi Fizike* (Proceedings of the Sixth School-Symposium on Chemical Physics) (Moscow: Moscow Aviation Technological Institute, 1994) p. 154
143. A S Kaklyugin *Khim. Fiz.* **13** (11) 102 (1994)
144. S Novak, M Collaud, G Dietler, P Groning, L Schlapbach *J. Vac. Sci. Technol. A* **11** 481 (1993)
145. M Kardar, G Parisi, Y C Zhang *Phys. Rev. Lett.* **56** 889 (1986)
146. D E Wolf, J Villain *Eur. Lett.* **13** 727 (1990)
147. J Villain *J. Phys. (France)* **1** 19 (1992)
148. Z-W Lai, S Das Sharma *Phys. Rev. Lett.* **66** 2348 (1991)
149. W H Tong, R S Williams, A Janase, Y Segawa, M S Anderson *Phys. Rev. Lett.* **72** 3374 (1994)
150. A Iwamoto, T Yoshinobu, H Iwasaski *Phys. Rev. Lett.* **72** 3374 (1994)
151. E K Grimmelman, J C Tully *J. Chem. Phys.* **74** 5300 (1981)
152. J C Keck *Adv. Chem. Phys.* **13** 85 (1967)
153. Z A Insepov, E M Karataev *Pis'ma Zh. Eksp. Teor. Fiz.* **17** (24) 36 (1991)
154. D Srivastava, B J Garrison *Phys. Rev. B* **46** 1472 (1992)
155. D Srivastava, B J Garrison *Phys. Rev. B* **47** 4464 (1993)
156. Z A Insepov, E M Karatajev, G E Norman *Z. Phys. D, At. Mol. Clusters* **20** 449 (1991)
157. Z A Insepov, E M Karatajev, G E Norman, in *Proceedings of the Workshop "Nucleations–Clusters–Fractals", Rostock University, Serrahn, 1991* p. 141
158. M I Haftel, M Rosen, T Franklin, M Hettermann *Phys. Rev. Lett.* **72** 1858 (1994)
159. F DeVita, I Štich, M J Gillan, M C Payne, L J Clarke *Phys. Rev. Lett.* **71** 1276 (1993)
160. S C Wang, G Ehrlich *Phys. Rev. Lett.* **71** 4174 (1993)
161. N Kitamura, M G Lagally, M B Webb *Phys. Rev. Lett.* **71** 2082 (1993)
162. M Shayegan, J M Cavallo, R E Glover III, R L Park *Phys. Rev. Lett.* **53** 1578 (1984)
163. J Stöhr, J L Gland, W Eberhardt, D Outka, R J Madix, F Sette, R J Koestner, U Doubler *Phys. Rev. Lett.* **51** 2414 (1983)
164. F M Hoffmann, R A dePaola *Phys. Rev. Lett.* **52** 1697 (1984)
165. G Jayaram, P Xu, L D Marks *Phys. Rev. Lett.* **71** 3489 (1993)
166. E I Asinovskii, L S Polak *Khim. Vys. Energ.* **28** 418 (1994)
167. H-J Ernst, F Fabre, R Folkerts, J Lapujoulade *Phys. Rev. Lett.* **72** 112 (1994)
168. M D Jonson, D Graff, J Sudijona, C Orme, A W Hunt, L M Sander, B J Orr *Phys. Rev. Lett.* **72** 116 (1994)
169. F Wu, S G Jaloviar, D E Savage, M G Lagally *Phys. Rev. Lett.* **71** 3489 (1993)